

# The Stellar Composition of the Star Formation Region CMa R1 – III. A new outburst of the Be star component in Z CMa <sup>\*</sup>

M.E. van den Ancker,<sup>1†</sup> P.F.C. Blondel,<sup>2</sup> H.R.E. Tjin A Djie,<sup>2</sup> K.N. Grankin,<sup>3</sup>  
O.V. Ezhkova,<sup>3,4</sup> V.S. Shevchenko,<sup>3,5</sup> E. Guenther<sup>6</sup> and B. Acke<sup>7‡</sup>

<sup>1</sup>European Southern Observatory, Karl-Schwarzschild-Strasse 2, D-85748 Garching bei München, Germany

<sup>2</sup>Astronomical Institute “Anton Pannekoek”, University of Amsterdam, Kruislaan 403, 1098 SJ Amsterdam, The Netherlands

<sup>3</sup>Astronomical Institute of the Academy of Sciences of Uzbekistan, Astromicheskaya 33, Tashkent 700052 Uzbekistan

<sup>4</sup>Sternberg Astronomical Institute, Moscow State University, Universitetskii Prospect 13, RU - 119899 Moscow, Russia

<sup>5</sup>Deceased March 2000

<sup>6</sup>Thüringer Landessternwarte Tautenburg, Sternwarte 5, D-07778 Tautenburg, Germany

<sup>7</sup>Astronomical Institute, Katholieke Universiteit Leuven, Celestijnenlaan 200B, B-3001 Heverlee, Belgium

Accepted <date>. Received <date>

## ABSTRACT

We report on a recent event in which, after more than a decade of slowly fading, the visual brightness of the massive young binary Z CMa suddenly started to rise by about 1 magnitude in December 1999, followed by a rapid decline to its previous brightness over the next six months. This behaviour is similar to that exhibited by this system around its eruption in February 1987. A comparison of the intrinsic luminosities of the system with recent evolutionary calculations shows that Z CMa may consist of a  $16 M_{\odot}$  B0 IIIe primary star and a  $\sim 3 M_{\odot}$  FUor secondary with a common age of  $\sim 3 \times 10^5$  yr. We also compare new high-resolution spectra obtained in Jan. and Feb. 2000, during the recent rise in brightness, with archive data from 1991 and 1996. The spectra are rich in emission lines, which originate from the envelope of the early B-type primary star. The strength of these emission lines increased strongly with the brightness of Z CMa. We interpret the collected spectral data in terms of an accretion disc with atmosphere around the Herbig B0e component of Z CMa, which has expanded during the outbursts of 1987 and 2000. A high resolution profile of the 6300 Å [O I] emission line, obtained by us in March 2002 shows an increase in flux and a prominent blue shoulder to the feature extending to  $\sim -700$  km s<sup>-1</sup>, which was much fainter in the pre-outburst spectra. We propose that this change in profile is a result of a strong change in the collimation of a jet, as a result of the outburst at the start of this century.

**Key words:** circumstellar matter – stars: emission-line – stars: pre-main sequence – stars: Z CMa – stars: variables – open clusters and associations: CMa R1

## 1 INTRODUCTION

Ever since the discovery of bright emission lines in its spectrum by Merrill (1927), Z CMa (HD 53179, IRAS 07013–1128) has been one of the most frequently studied

<sup>\*</sup> Based on observations made with the European Southern Observatory telescopes obtained from the ESO/ST-ECF Science Archive Facility, with the William Herschel Telescope operated on the island of La Palma by the Isaac Newton Group in the Spanish Observatorio del Roque de los Muchachos of the Instituto de Astrofísica de Canarias, with the BTA telescope of the Special Astrophysical Observatory, Nizhnii-Arkhyz, Russia, and with the Alfred Jensch telescope of the Thüringer Landessternwarte, Germany.

<sup>†</sup> Visiting Astronomer at the Infrared Telescope Facility, which is

operated by the University of Hawaii under Cooperative Agreement no. NCC 5-538 with the National Aeronautics and Space Administration, Office of Space Science, Planetary Astronomy Program.

<sup>‡</sup> E-mail contact: Herman Tjin A Djie (herman@science.uva.nl)

massive young stars. The brightness of the system is highly variable, varying irregularly between its quiescent state at  $V \approx 11$  to its active state at  $V \approx 9$  (Covino et al. 1984; Hessman et al. 1991). Although the photometric and spectroscopic properties of Z CMA show some similarity with those of the FUors (e.g. FU Ori and V1057 Cyg), its spectral differences with these objects, especially in the presence of many narrow emission lines, are remarkable. Nevertheless, in its normal brightness phases ( $V > 9.6^m$ ) the absorption character of the spectrum is dominant and, similar to the FUors, the spectrum can be interpreted as that of an optically thick accretion disc (Hartmann et al. 1989; Welty et al. 1992).

In Feb. 1987 a large rise in brightness of Z CMA was accompanied by a rise in emission flux in the Balmer lines and Ca II K and with the transition of many metal lines of Fe II, Cr II and Ti II from absorption into emission (Hessman et al. 1991). These authors tried to explain the absorption and emission spectral components in terms of a common source, a variable accretion disc. However, it proved difficult to find a simple model for such a source that would be able to reproduce the observations. A key ingredient in solving this mystery was discovered in 1989, when near-infrared speckle interferometry revealed that Z CMA is a double star with a separation of  $0.1''$  (Koresko et al. 1991; Haas et al. 1993). These authors showed that the South-Eastern component of Z CMA dominates the visual and UV parts of the SED and is associated with a FUor-like system, whereas the North-Western component is a powerful infrared source, which is the primary object of this double star system. The separation of Z CMA into two components has since been confirmed by speckle masking observations in the visual ( $R$ -band) by Barth et al. (1994) and by Thiébaud et al. (1995). In addition it was discovered by Whitney et al. (1993) that the emission lines in the visual part of the spectrum of Nov. 1991 were polarized, in contrast to the continuum of the spectrum. This supports the idea that these emission lines are contributed by scattered light from the primary source of the system.

The analogy of this spectrum with that of the early type Herbig Be star MWC 1080 suggests that the source of the emission lines is an early type Be star inside a large cocoon. The radiation of this Be star escapes by scattering from the dust walls of a cavity in the thick cocoon envelope. Millan-Gabet & Monnier (2002) successfully imaged the direct circumstellar environment of Z CMA at  $1.25 \mu\text{m}$ , and found a small ( $\sim 1''$ ) linear feature. They interpreted this feature as light scattered off the walls of a jet-blown cavity, confirming the above picture. The cavity could be formed by the extended (over 3.6 pc) optical jet discovered by Poetzl et al. (1989). This jet is also seen as a bipolar outflow in CO (Evans et al. 1994). More recent spatially resolved optical spectroscopy by Bailey (1998) and Garcia et al. (1999) has confirmed that the extended outflow originates from the infrared primary component of Z CMA and that the optical emission line spectrum is associated with the same component.

During Nov./Dec. 1999, observers of the ROTOR photometric monitoring program at Mt. Maidanak Observatory (Uzbekistan) found that after seven years of low brightness ( $V \sim 10.3^m$ ) the brightness of Z CMA rose sharply (within 40 days) by more than 1 magnitude. We obtained new high-resolution spectra of Z CMA shortly after this new outburst.

These spectra show intrinsic changes in line profiles and equivalent widths with respect to spectra obtained in 1991 and 1996. In this paper we discuss the spectral changes of Z CMA over the last ten years and interpret these changes as due to changes in the size of an accretion disk, associated with the Herbig B0e primary.

From *UBVRI* photometry of Z CMA obtained in Nov. 1991 and Feb. 1987 (Sect. 3.2) we confirm the spectral classification of the star in the primary source and derive its radius and luminosity for spectral type B0III. Although the photometric data of Z CMA suggest that the variability of the contributions from both binary components is for a large part due to irregular variations in their circumstellar dust extinctions (Sect. 3.1), there are variations in the spectrum of the Be component which show that intrinsic changes of the Be envelope excitation occur and possibly also influence the circumstellar extinction.

In Sect. 4 we discuss the formation regions of the various emission lines, and note that several strong absorption lines from He I, O I and part of the Na I D lines can also be attributed to the B0e star. From the red Ca II (2) emission line triplet and various multiplets of Fe II emission lines we have estimated lower limits to the disc radius of the ‘hidden’ Herbig Be star. We also make estimates of the outflow and accretion rates of the Be star.

In the discussion (Sect. 5) we compare our data of Z CMA with those of three Herbig stars with similar spectra: MWC 1080, V645 Cyg and V380 Ori. We also make some attempts to estimate the evolutionary stage and mass of the B0e star from recent models for the pre-main sequence evolution of massive stars. It appears possible to find models for the two components of Z CMA which predict the accretion rates (derived from the observations) and which also predict a bipolar jet only for the B0e star.

## 2 OBSERVATIONS

### 2.1 Photometry

Since 1980 Z CMA has been monitored closely in the Johnson *UBVR* system by the ROTOR photometric monitoring program. The observations in this program were made with three different 0.6 m telescopes at Mt. Maidanak Observatory, Uzbekistan. During these observations, mostly made through a  $15''$  circular diaphragm, the telescope was equipped with a single-channel photometer. Standards and extinction reference stars were observed each night. The data were reduced with standard techniques at the Tashkent Astronomical Institute. A detailed description of the ROTOR program and the employed measuring procedures can be found in Shevchenko (1989).

The ROTOR data on Z CMA were supplemented with optical and infrared measurements on various photometric systems from the literature. When possible, all data were transformed to the ‘standard’ Johnson/Cousins *UBVR<sub>C</sub>IC* and near-infrared *JHKLM* systems using the transformation formulae from Fernie (1983), Brand & Wouterloot (1988), and Carpenter (2001). The results are given and discussed in Sect. 3.1.

**Table 1.** Log of spectroscopic observations of Z CMa. We also list the  $V$ -band photometric measurement closest to the date of each spectroscopic observation.

Telescope	Range [Å]	Date	JD+2400000	$R$ [mÅ]	$t_{\text{exp}}$ [min]	$V$ [mag]
SAO 6 m	4190–5490	22 Nov. 1991	48582.83	300	–	9.7
SAO 6 m	5960–7150	23 Nov. 1991	48583.83	300	–	9.7
ESO NTT	5720–9930	20 Dec. 1991	48610.838	279.5	20	9.8
ESO NTT	5720–10030	21 Dec. 1991	48611.710	279.5	45	9.8
ESO 1.5 m	4200–7800	6 Dec. 1992	48962.823	1076	4	10.3
ESO 1.5 m	6200–8700	10 Dec. 1992	48966.651	747	8	10.3
ESO CAT	5860–5910	15 Dec. 1994	49701.355	107.0	45	10.2
ESO CAT	6521–6600	12 Dec. 1996	50429.151	65.6	45	10.2
ESO CAT	5848–5918	13 Dec. 1996	50430.210	58.8	45	10.2
ESO CAT	5848–5918	14 Dec. 1996	50431.235	58.8	45	10.2
ESO CAT	3913–3955	14 Dec. 1996	50431.323	39.3	45	10.2
ESO CAT	8467–8573	15 Dec. 1996	50432.235	85.2	45	10.2
WHT	5220–9110	26 Dec. 1996	50443.725	266.7	20	10.3
WHT	5220–9110	26 Dec. 1996	50443.740	266.7	20	10.3
Tautenburg 2 m	5600–10050	23 Jan. 2000	51567.422	230.0	20	9.1
WHT	3640–5470	18 Feb. 2000	51593.361	177.2	30	9.2
WHT	4100–8350	18 Feb. 2000	51593.423	232.0	30	9.2
WHT	4600–9960	18 Feb. 2000	51593.447	278.4	30	9.2
WHT	5330–11020	18 Feb. 2000	51593.498	325.8	30	9.2
NASA IRTF	19000–41400	18 Dec. 2001	52262.139	32.0	5	10.0
ESO 3.6 m	6279–6321	31 Mar. 2002	52365.084	42.0	30	10.0

## 2.2 Spectroscopy

In this paper we present the spectra of Z CMa obtained with a range of telescopes:

(a) Two low resolution spectra, taken on 9 and 10 December 1992 with the Boller and Chivens spectrograph on the 1.5 m telescope at ESO’s La Silla Observatory. These spectra show emission in  $H\alpha$ , [O I] 6300 Å, O I 8446 Å and Ca II (2) (8500, 8545 and 8662 Å). The emissions of  $H\beta$ , P14 and Fe II (42), which are clear in the low resolution spectrum of the B5 star LkH $\alpha$  220 (Tjin A Djie et al. 2001 (hereafter paper II), Fig. 5) are much weaker in this spectrum of Z CMa. In contrast, the emission lines in the Z CMa spectra of Whitney et al. (1993, Fig. 1). of Nov. 27, 1991 are stronger than those of LkH $\alpha$  220.

(b) A high resolution blue spectrum (4190–5490 Å) obtained with the Main Spectrograph on the 6 m BTA telescope of the SAO (Special Astrophysical Observatory in Nizhnii-Arkhyz) on 22 Nov. 1991 and a high resolution  $H\alpha$  profile obtained with the same instrument on 23 Nov. 1991. Similar to the spectrum of Whitney et al. (1993), which was taken a few days later, the SAO spectrum shows strong emission components in  $H\alpha$ ,  $H\beta$ ,  $H\gamma$  and in several multiplets of Fe II. These spectra are supplemented by high resolution red *ESO Multiple-Mode Instrument* (EMMI) spectra, obtained on 20 and 21 Dec. 1991 with the 3.5 m *ESO New Technology Telescope* (NTT) and extracted by us from the ESO science archive.

(c) High resolution echelle spectra have been secured with the *Coudé echelle spectrograph* (CES) mounted on the 1.4 m *Coudé Auxiliary Telescope* (CAT) at La Silla: (1) Na I D absorption profiles of Dec. 15, 1994 and of Dec. 13 and 14, 1996 (2) An  $H\alpha$  emission profile of Dec. 12, 1996 (3) A Ca II K emission and absorption profile of Dec. 14 1996 (4) Ca II (8498 Å) and Ca II (8542 Å) (blended with resp. P16 and P15) emission profiles of Dec. 15, 1996. Addition-

ally, an emission profile of the [O I] 6300 Å line has been obtained with the same instrument connected to the ESO 3.6 m telescope on March 31, 2002.

(d) A high resolution red spectrum (5470–9110 Å) taken on Dec. 26, 1996 (close to the dates of the observations mentioned under c) with the *Utrecht Echelle Spectrograph* (UES) on the 4.2 m WHT at the Northern Hemisphere Observatory on La Palma was kindly made available to us by Drs. H. van Winckel and G. Meeus of the Katholieke Universiteit Leuven (Belgium).

(e) A high resolution red spectrum (5600–10050 Å) was obtained on January 23, 2000 with the *Coudé Echelle Spectrograph* of the 2 m Alfred Jensch telescope of the Thüringer Landessternwarte ‘Karl Schwarzschild’ in Tautenburg, Thüringen. This spectrum was taken during a very bright phase of Z CMa ( $V \sim 9.1^m$ ), comparable to the outburst of Feb. 1987 ( $V \sim 8.7^m$ ). The spectrum covers the wavelength range from about 560 to 1005 nm. Using a Tek CCD Chip with  $1024 \times 1024$  pixels and a slit-width of two arcseconds, the two-pixel resolution of the spectrum is about  $\lambda/(\delta\lambda) = 35,000$ . Standard IRAF routines were used in order to extract and wavelength calibrate the spectrum.

(f) Four high resolution echelle spectra, centered at 4300 Å, 5200 Å, 6200 Å and 8200 Å were obtained on Feb. 18, 2000 with the UES on the 4.2 m WHT. A number of line profiles from these spectra will be compared with the corresponding profiles from the spectra mentioned under (b)–(e) and with those published in the literature. Apart from the blue range, these spectra extend in the red up to 11020 Å. However, some lines (e.g. [O I] 6300 Å) could not be observed in these spectra because there is no wavelength overlap of the successive orders.

(g) A near-infrared (1.9–4.1  $\mu\text{m}$ ) spectrum has been taken with the SpeX spectrograph (Rayner et al. 2003) attached to the 3.0 m *NASA Infrared Telescope Facility* (IRTF) of the Mauna Kea Observatory on Dec. 18, 2001.

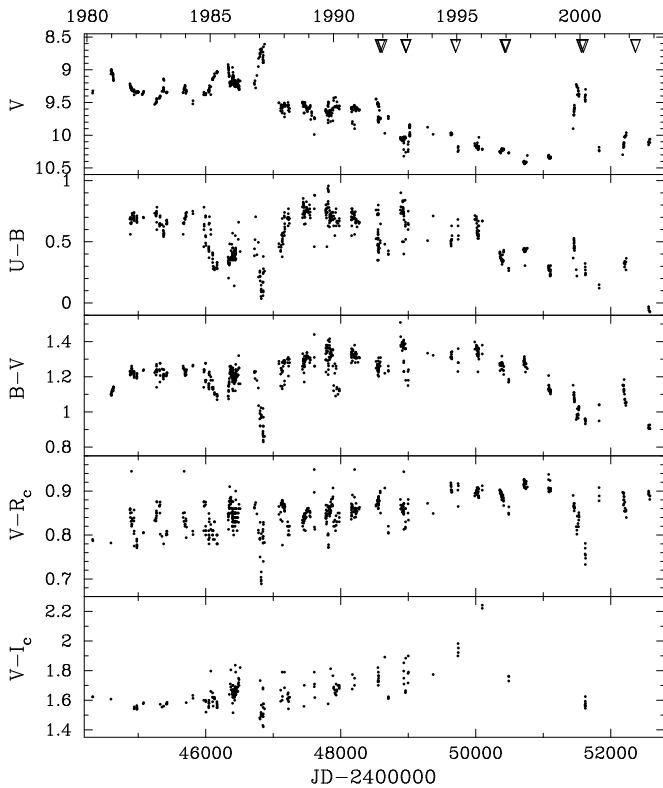


**Figure 1.** Optical ( $UBVR_cI_c$ ) light-curve of Z CMa spanning the period 1980–2003. Typical errors in magnitude and colours are of the order of 0.02 mag. The triangles in the top panel indicate the dates of the spectroscopic observations listed in Table 1.

In this spectrum we observe Br  $\alpha$ , Br  $\gamma$ , Pf  $\gamma$  and several CO lines in emission.

Observational details of all spectroscopic observations are reviewed in Table 1.

### 3 PHOTOMETRY AND INTERPRETATION

#### 3.1 Variability and Lightcurve

Figures 1 and 2 show the optical ( $UBV(RI)_C$ ) and near-infrared ( $JHK$ ) lightcurve of Z CMa between 1980 and 2003. For a detailed description of the photometric behaviour of Z CMa before the 1987 outburst, we refer the reader to the papers of Covino et al. (1984), Hessman et al. (1991), and Lamzin et al. (1998). From Fig. 1 we conclude that whereas before 1987 the system brightness appears relatively constant, from Feb. 1987 to Dec. 2000 the brightness of the star is steadily declining by about  $0.1^m$  per year. Clear variability is seen superimposed on this trend, such as a local minimum around December 1992. There appears to be a strong correlation between the observed brightness and colour variations in Z CMa. We illustrate this point in Fig. 3, where we give the  $V$  vs. ( $U - B$ ), ( $B - V$ ), ( $V - R_c$ ) and ( $V - I_c$ ) distributions for the time-interval 1980–2003. Although some correlation is present in these diagrams, the spread of the data-points is much larger than expected from the observational errors ( $\sim 0.02^m$ ).

A closer inspection shows that between Feb. 1987 and

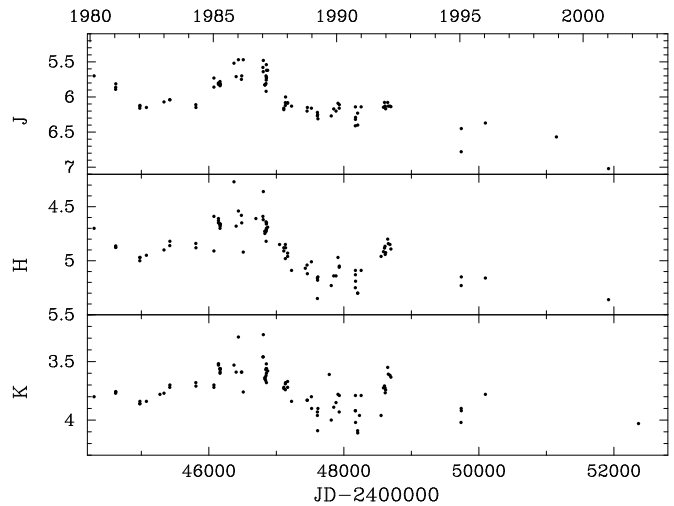


**Figure 2.** Near-Infrared ( $JHK$ ) light-curve of Z CMa spanning the period 1980–2003. Typical errors in these data are about 0.05 mag.

Nov. 1991 the photometric variations closely follow a behaviour of redder colours when the system gets fainter, but that the data of Dec. 1999 and March 2001 are shifted to somewhat lower values of ( $B - V$ ) and ( $U - B$ ) than defined by the reddening line. We infer that either variable circumstellar extinction or a slow cooling-down of the FUor component in Z CMa may explain the long-term overall trend of the photometric variation between Feb. 1987 and Dec. 2000. However, on a shorter time-scale of weeks and days the variations seem erratic and hard to explain. This may not be surprising, since we probably are observing the result of two independently varying sources, a FUor secondary component which usually dominates the visual continuum and a Be type primary star in a large dust cocoon, which is dominating the near and far infrared part of the spectrum (Koresko et al. 1991). Fig. 2, displaying the variation of the near-infrared magnitudes, shows that in 1991 the  $H$  and  $K$  band fluxes reach a local maximum, which is more pronounced than that in the  $V$  band. This suggests that the circumstellar extinction of the cocoon around the primary component has decreased so far, that the visual flux from that component could increase its contribution to the total flux in the visual somewhat.

Apart from the long-term variations discussed above, the dominant features in the optical light-curve of Z CMa are the large and fast rises in visual flux in Feb. 1987 and Jan. 2000 (Fig. 1). The latter maximum started with a fast rise, first observed in Oct. 1999, over  $0.7^m$  in  $V$  taking 46 days. The star remained at this high brightness for at least 180 days. When extrapolating to earlier dates, the total increase in  $V$ -brightness is  $\sim 1.1^m$ , but the time-scale of this larger variation has not been observed. The time-scale of the rise in brightness over  $0.7^m$  during Jan./Feb. 1987 is also not known, but the duration of the higher brightness phase was also about 6 months (Hessman et al. 1991, Fig. 1).

We note that the large and fast rises in the visual fluxes in Feb. 1987 and Jan. 2000, do not originate in a large, fast decrease in circumstellar extinction; it will be shown by

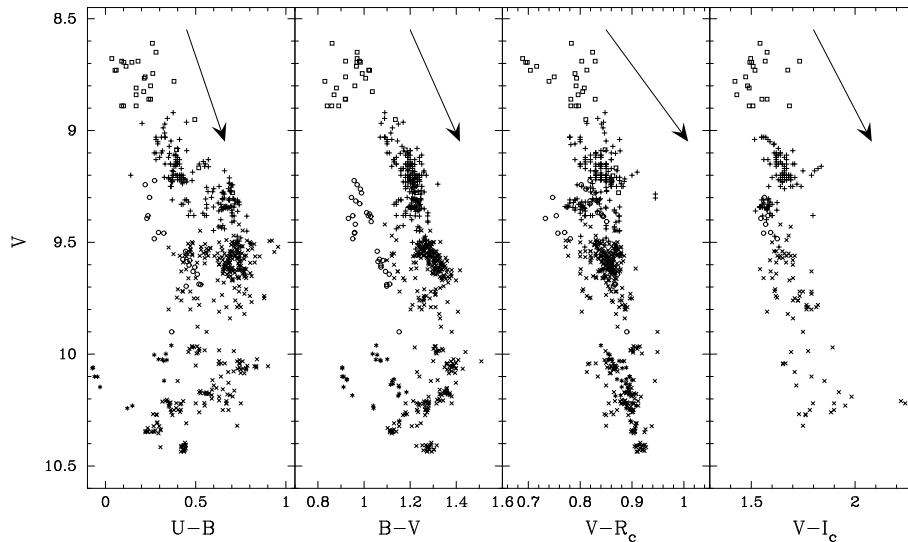


**Figure 3.** Optical ( $UBVR_cI_c$ ) colour-magnitude diagram of Z CMA using photometric data from the period 1980–2003. Data from Jan. 1980–Jan. 1987 are indicated by the plusses, data from the Feb. 1987 outburst by open squares, data from Mar. 1987–Oct. 1999 by the crosses, data from the Nov./Dec. 1999 outburst by the open circles, and data points obtained after Feb. 2000 are indicated by the asterisk symbols. The arrows indicate the direction of interstellar reddening

the spectroscopy (Sect. 4) that they are related to intrinsic changes of the primary Be star component.

### 3.2 The SEDs in the visual

From the spectral polarization data measured in Nov. 1991 by Whitney et al. (1993), the authors derived that at this date 75% of the visual flux was contributed by the FUor secondary source and that the remaining 25% was due to the Be-type primary star. By assuming that the fast rise in visual brightness of Feb. 1987 (Hessman et al. 1991) was entirely due to a rise in the primary brightness only, they derived that on Feb. 19, 1987 the contribution of the primary Be star to the total visual flux was 66%. In the same way we derive from the fast rise in Nov./Dec. 1999 that at maximum brightness in Jan. 2000 ( $V \sim 9.1^m$ ) the contribution of the primary Be star to the total visual flux was  $\sim 60\%$ .

In the UV the spectrum is dominated by the FUor companion. Earlier obtained UV spectra could be matched with a model of an accretion disc with a late F-type spectrum (Hartmann et al. 1989; Kenyon et al. 1989). We have made a similar fit of two IUE spectra (taken on 17 April 1979 when  $V \sim 9.3^m$  and 19 March 1988 when  $V \sim 9.6^m$ ). Good fits were obtained with a F5Ib star, an  $0.02 R_*$  thick boundary layer with  $T_{\text{eff}} = 10,500$  K and an optically thick disc with 5400 K maximum temperature. We assumed a foreground excess of  $0.16^m$  with  $R_{\text{is}} = 3.1$  and a foreground CMA R1 cluster excess of  $0.20^m$  with  $R_{\text{cs}} = 4.2$  (Shevchenko et al. 1999; Paper I). The accretion rate for the FUor is then  $\sim 3 \times 10^{-5} M_{\odot} \text{ yr}^{-1}$ .

From the observed  $UBVRI$  photometry, the above mentioned foreground excess and the relative flux contributions of a B0III primary and a FUor (F5Ib) secondary component we have calculated the extinction-free  $UBVRI$  fluxes of both components in 1987, 1991 and 2000 for various values of  $R_{\text{cs}}$  (3.1, 4.2 and 6.0). We assumed here intrinsic colours  $(B-V)_0 = -0.29^m$  for a B0III star and  $(B-V)_0 =$

**Table 2.** Radii and luminosities of the B0IIIe star on 20 Feb. 1987, 23 Jan. 2000, and 22 Nov. 1991 for  $R_{\text{cs}} = 3.1$ ,  $R_{\text{cs}} = 4.2$  and  $R_{\text{cs}} = 6.0$ . The uncertainties in the computed values of  $R/R_{\odot}$  and  $\log(L/L_{\odot})$ , dominated by the 14% error in the distance to CMA R1 (paper I), are less than 10% and 3 around a few thousand K.

Obs. Date	$V_{\text{obs}}$ [m]	$R_{\text{cs}}$	$V_0$ [m]	$R/R_{\odot}$	$\log(L/L_{\odot})$	$T_{\text{eff}}$ [K]
02/20/87	8.8	3.1	5.39	12.3	4.81	26,000
01/23/00	9.2	3.1	5.70	10.6	4.68	26,000
11/22/91	9.8	3.1	6.14	8.0	4.57	28,000
02/20/87	8.8	4.2	4.50	18.5	5.16	26,000
01/23/00	9.2	4.2	4.72	16.7	5.07	26,000
11/22/91	9.8	4.2	4.80	16.1	5.04	28,000
02/20/87	8.8	6.0	3.03	33.6	5.81	28,000
01/23/00	9.2	6.0	3.12	32.4	5.78	28,000
11/22/91	9.8	6.0	2.61	37.5	6.01	30,000

$0.37^m$  for the FUor (Schmidt-Kaler 1982). The extinction-free  $UBVRI$  distributions of the B-type primary star can be matched with the Kurucz model flux ratios of a late O or early B-type star, which gives us an effective temperature, a radius and a luminosity for each of the dates of spectroscopic observations (Table 2). We will use these results in Sect. 4 and in the discussion on the evolutionary status of Z CMA (Sect. 5).

In reality the values of  $R/R_{\odot}$  and  $\log(L/L_{\odot})$  of Table 2 may be somewhat higher because so far we have not accounted for the fact that we only receive the light from the star after it has been scattered and polarized by the dust walls of the cavity in the cocoon. The correction for this reduction is uncertain, but because of the upper limit of 10% for the degree of polarization (Whitney et al. 1993) we estimate that the scattering angle will not be larger than 20 degrees, so that the flux reduction due to scattering will not

be more than 5% if the scattering grains are more or less aligned (see Figs. 8 and 9 of the paper of Voshchinnikov & Farafonov 1993). Our estimate that the scattering angle is small is supported by the relatively large radial velocities of the [N II] and [S II] emission lines in the bipolar outflow along the axis of the cavity (Poetzel et al. 1989).

### 3.3 The mass loss of the Be primary component

From Jan. 1981 Z CMa photometry on the Walraven *WULBV* system (de Winter et al. 2002) we can make an estimate of the mass loss from the early Be-type companion. After transformation of the flux in the Walraven *V*-band to the Johnson system we find that the visual magnitude in this period was  $9.0^m$ , which suggests that the continuum of the B star dominated the visual part of the spectrum at that date. After correction for foreground extinction, the Balmer jump  $D_B$ , derived from the Walraven photometry is  $0.16^m$ . Predicted values of the Balmer jump based on model calculations by Mihalas (1966) can be found in Fig. 2 of the paper of Garrison (1978). For B0 and  $\log g = 3$  the theoretical value of the Balmer jump is close to  $0.15^m$ , but for  $\log g = 4$  the predicted value is already  $0.29^m$ , which implies that  $\Delta D_B$  for B0III has an upper limit of  $0.13^m$ . We estimate the mass loss with the method of Garrison and assume a temperature of 10,000 K for the outflow region. Then the upper limit of  $\Delta D_B$  leads to an upper limit of  $1.6 \times 10^{37} \text{ cm}^{-6}$  for the volume emission measure and with an outflow velocity of  $1000 \text{ km s}^{-1}$  in the  $H\alpha$  emission region (see Sect. 4) and a radius of  $9.4 R_\odot$  we have an upper limit of  $1 \times 10^{-4} M_\odot \text{ yr}^{-1}$  for the mass loss in the wind. The mass loss is proportional with the outflow velocity in the emission region, so that the actual upper limit can easily be twice as low.

## 4 ANALYSIS OF THE SPECTRA

### 4.1 Results

Table 4 gives the data of the lines in the red spectra (longward  $5650 \text{ \AA}$ ) in the Z CMa spectra for  $V \sim 9.1^m$ , for  $V \sim 9.7^m$  and for  $V \sim 10.3^m$ . The tables contain equivalent widths (EWs), half-widths (FWHM) and P Cygni outflow velocities of the lines. In Tables 3 the corresponding data of the lines in the blue spectra are listed.

In order to learn more about the structure of the envelope of the early Be type primary we discuss the various lines and their profiles in the high resolution red and blue spectra of Jan. and Feb. 2002 ( $V \sim 9.1^m$ ) and then compare the results with the corresponding red and blue spectra, observed in Nov. (blue) and Dec. (red) 1991 ( $V \sim 9.6^m$ ), and with the profiles of several characteristic lines, secured in Jan. 1996 ( $V \sim 10.2^m$ ).

### 4.2 The outburst spectra of 2000 and 1987

#### 4.2.1 The emission lines

In discussing the lines we first should know of which stellar component they originate. The presence of N I (8629 and  $8683 \text{ \AA}$ ) emission is an indication for a hot atmosphere, since the lines have been only observed for (early) B stars

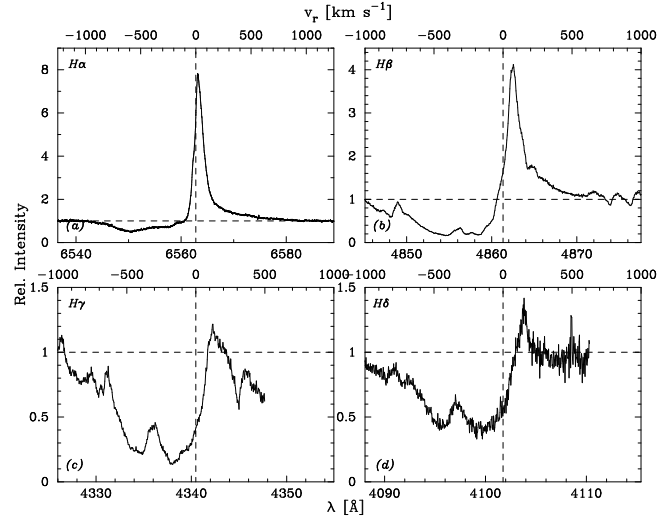


**Figure 4.** H I Balmer line profiles of Z CMa. (a)  $H\alpha$  line profile obtained on 12 Dec. 1996, (b)  $H\beta$  profile obtained on 18 Feb. 2000, (c)  $H\gamma$  profile obtained on 18 Feb. 2000, (d)  $H\delta$  profile obtained on 18 Feb. 2000. The dashed horizontal and vertical lines indicate the continuum level, and the rest-wavelength of the observed line, respectively.

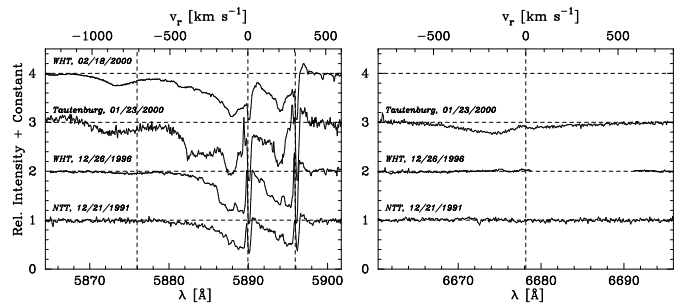


**Figure 5.** Na I and He I line profile variations in Z CMa between 1991 and 2000. The left panel shows the  $5889.95$  and  $5895.92 \text{ \AA}$  Na I D lines, together with the  $5875.97 \text{ \AA}$  He I line, whereas the right panel shows the spectral region around the  $6678.15 \text{ \AA}$  He I line. Strong He I absorption is only present in the Jan. and Feb. 2000 spectra.

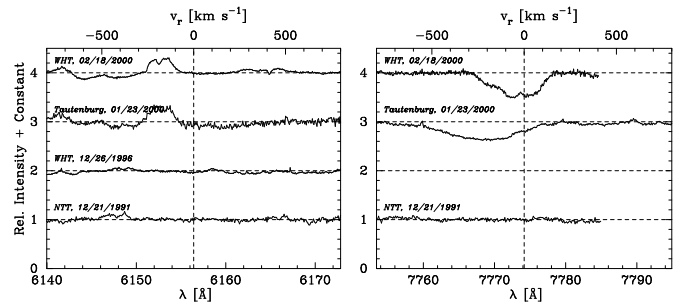


**Figure 6.** O I line profile variations in Z CMa between 1991 and 2000. The left panel shows the observed variability in the O I  $6156.41 \text{ \AA}$  line, whereas the right-hand panel illustrates the behaviour of the O I  $7774.17 \text{ \AA}$  line.

(Hamann & Persson 1992b). Similarly strong, high excitation Fe II 9997.57 Å emission has only been observed in spectra of early Be type stars, such as  $\gamma$  Cas (B0IV) (Viotti et al. 1998). This line is probably formed by fluorescence due to pumping by Ly $\alpha$  (see e.g. Rodríguez-Ardila et al. 2002). Whitney et al. (1993) and Garcia et al. (1999) have shown that the emission lines are associated with the primary Be-star. The main part of this emission will come from the extended envelope of this star, but the forbidden lines of [N II], [S II] and [O I] have been shown to be formed in the bipolar outflow (or a jet) from the primary (Poetzel et al. 1989; Garcia et al. 1999). From spectral imaging Bailey (1998) revealed that also a substantial part of the central region of the H $\alpha$  emission is emitted by the jet. The peak of the line is redshifted by +82 km s<sup>-1</sup> with respect to the laboratory wavelength. The wings of the line have their origin in the extended atmosphere of the primary Be-star. Especially the red wing extends very far, up to nearly 1000 km s<sup>-1</sup>. The emission peak of H $\beta$  shows a similar redshift of +75 km s<sup>-1</sup>.

We assume that the other Balmer (and Paschen) lines will be formed in the same region as H $\alpha$ . A strong argument in favour of this is that all Balmer lines (from H $\alpha$  to H15) in the WHT spectrum have a similar outflow velocity pattern. From the last resolved Balmer lines ( $n \sim 35$ ) we derive from the Inglis-Teller relation that  $n_e \lesssim 2.4 \times 10^{11}$  cm<sup>-3</sup> in the region of their formation. For the Paschen lines, which have strong emission components (lower continuum in red part of the spectrum),  $n = 23$  which corresponds to  $n_e \approx 10^{13}$  cm<sup>-3</sup>.

The emission line of O I at 8446.5 Å is expected to be correlated with the H $\alpha$ -emission, because the  $3d^3D^0$  state of O I, which can be pumped by Ly $\beta$  (Polidan & Peters 1976), cascades down successively by the emission of 11291 Å to  $3p^3P$ , that of 8446 Å to  $3s^3S^0$  and finally by that of 1302 Å to the  $3P$  ground state. Its EW varies from negligible at Apr. 1989 ( $V \sim 9.7^m$ ) to 1.6 Å in Dec. 1987 ( $V \sim 9.5^m$ , Hamann & Persson 1992b), 1.2 in Dec. 1991 ( $V \sim 9.6^m$ ), 1.5 Å in Jan. 1996 ( $V \sim 10.2^m$ , Teodorani et al. 1997) to 1.4 Å on Jan 2000 ( $V \sim 9.1^m$ ). For the last three dates, the EW of H $\alpha$  varied from 19.1, 32.5 to 42.2 Å which does not seem to confirm the expected correlation between the EWs of O I and H $\alpha$  for Z CMa. It should be kept in mind though that the H $\alpha$  emission peak contains an unknown component, which is emitted by the outflow region (Bailey 1998). The variation of the H $\alpha$  emission EW is therefore partly due to variation in the outer atmosphere, whereas the emission of O I (8446.5 Å) originates in the inner part of the atmosphere.

Next to the Balmer emission lines, the Ca II (2) triplet lines have by far the strongest emission fluxes in the spectra of Z CMa. Although the three lines are blended by the Paschen lines P16, P15 and P14, the contributions from these lines to the flux are small (their EWs are about 5% of the total EW). The lines have P-Cygni profiles with outflow velocities around 500 km s<sup>-1</sup> and half-widths of 107, 110 and 132 km s<sup>-1</sup> for 8498, 8542 and 8662 Å respectively. The line shapes are very asymmetrical: the red wings extend to more than 8 Å from the line center, which suggests that the lines are formed in a turbulent region.

We confirm the presence of many emission lines from Fe II of multiplets 27, 28, 32, 35, 36, 37, 38, 40, 42, 43, 46, 48, 49, 55, 73, 74 and 199, several lines of Cr II multiplet 30, 43 and 44 and a few lines of Ti II (20) and Sc II (29). Apart

from multiplet 73 in the red part of the spectrum, most of these lines are also given in the line list of the high state spectrum of Hessman et al. (1991). We discuss the variation of the Fe II lines in Sect. 4.6. In the red part of the spectrum we also observed fairly strong emission of the lines of Fe I multiplet 60.

#### 4.2.2 Source of the broad absorption troughs of He I and O I

The lines of He I (7065, 6678 and 5876 Å) (Fig. 5) and O I (7773 and 6156 Å) (Fig. 6) have relatively broad absorption features. They also show a weak emission at a small redshift (+65 km s<sup>-1</sup>) from the laboratory wavelength and a broad (-450 km s<sup>-1</sup>) blueshifted absorption trough and therefore have the shape of P Cygni profiles. There are several reasons to believe that these profiles are formed in the envelope of the primary Herbig B0e star: In Fig. 10 of the paper by Hessman et al. (1991) we see that in the post-eruption phase the 6678 Å He I singlet line has disappeared and replaced by two Fe I lines with the double structure which is characteristic for the FUor component. The broad profile for the high state (in the same Fig. 10) shows only weak indications of these double lines, which suggests that during this state the continuum of the primary star is higher than that of the secondary FUor component (see also Sect. 3.2), so that the absorption line contribution from the primary (Be) component is dominating. In fact it was estimated by Whitney (1993) that in the high state the contribution of the FUor component to the visual continuum is only one third of the observed continuum and therefore one half of the contribution by the primary Be star.

The 7065 Å and 5876 Å He I triplet lines in the Tautenburg spectrum show the same profiles as that of the 6678 Å He I singlet line. Although the 6678 Å line is outside the orders of the WHT spectrum, we can see from the comparison of the Tautenburg and WHT spectra that the profile of the 5876 Å line is the same in both spectra, so that the He I line did not change over a period of one month, in contrast to the neighbouring Na I profiles. Because of its high excitation energy (23 eV), the emission components in the He I lines will originate from the hot neighbourhood of the stellar surface. The broad blue-shifted absorption components must be interpreted as a strong and fast outflow with a broad (perhaps turbulent) velocity spectrum. We also note here that no line of He II (e.g. 4686 Å) was found in our optical spectra so that there are no direct indications for the presence of a chromosphere or transition region.

The O I (7773 Å) triplet has been observed in absorption for several Herbig Ae/Be stars (Felenbok et al. 1988; Hamann & Persson 1992b). In Z CMa, this line shows indications of emission components, redshifted by  $\sim 70$  km s<sup>-1</sup> and the absorption components are very similar to that of the 6678 Å He I line. This indicates that the line is not necessarily formed by the FUor component. It is also clear that in Jan. 2000 the continuum of the primary B0e star was much higher than that of the FUor at the time of the observation.

Hamann & Persson (1992b) suggest that the O I profile is formed in a highly turbulent envelope region. This may also be concluded from spectral surveys over many stars with different spectral and luminosity class (e.g. Slettebak 1986; Jaschek et al. 1993). These authors show that the only

early B-type stars with O I (7773 Å) in absorption are the shell stars. In addition it has been shown by Faraggiana et al. (1988) that for this line EWs of the order of 2 Å are only found for stars of spectral type earlier than B1. For Z CMA the maximum velocity of the outflow is  $\sim 500 \text{ km s}^{-1}$  in the Tautenburg spectrum. Because the excitation potential of the O I lines is only 10.7 eV, the inner border of the turbulent region were the emission of O I is formed will be further away from the stellar surface than that of He I (6678 Å). The same profile as for the O I (7773 Å) triplet is found for the 6157 Å triplet of O I, which, when in emission, cascades down by 7773 Å emission from the  $3p^5P$  state to the metastable  $3s^5S^0$  state at  $\chi_i = 9.5 \text{ eV}$ .

#### 4.2.3 The Na I D, Ca II K and K I lines

The observed Na I D profiles (Fig. 5) consist of at least three components: a narrow absorption component, an emission component and a broad absorption component, composed of several blue-shifted lines. The narrow components of D<sub>1</sub> and D<sub>2</sub> are shifted by  $\sim 27 \text{ km s}^{-1}$ , which is close to the radial velocity of Z CMA. We assume that they are due to absorption by the foreground interstellar medium and the local CMA cloud. Their FWHM is  $\sim 24 \text{ km s}^{-1}$ . The EWs of the narrow components (Table 4) can be used to estimate the Na I foreground column densities with the help of the Strömberg (1948) doublet method. By assuming a galactic abundance ratio  $N(\text{H})/N(\text{Na})$  of  $5 \times 10^5$  we can derive an average interstellar gas column and, with the empirical relation of Hobbs (1974), we can obtain a value for  $E(B - V)$  of 0.32, which is in line with the foreground excesses of the other stars in CMA R1 (papers I and II).

In the high resolution spectra obtained at ESO ( $V \sim 10.2^m$ ) and Tautenburg ( $V \sim 9.1^m$ ), the emission components of the Na I D lines are narrow and on both sides of the narrow absorption components. We suspect that they are the emission components (intersected by the interstellar absorption lines) of Na I D P-Cygni profiles.

The deepest and narrowest absorption component extends from  $-30$  to  $-200 \text{ km s}^{-1}$  with respect to the interstellar component with a FWHM of  $65 \text{ km s}^{-1}$ . According to Whitney et al., the deep absorption component of the D-lines is associated with the secondary (FUor) component. It causes a strong increase in polarization of the combined spectrum over this wavelength interval because the deep Na I D absorption lines of the secondary source cannot dilute the polarized continuum emission of the primary. The deep absorption components around 5896 and 5886 Å ( $F/F_c \approx 0.2-0.3$ ) will therefore almost certainly be formed around the secondary star. This is very similar to the Na I D line profiles of the FUors FU Ori and V1057 Cyg (see e.g. Welty et al. 1992, Figs. 6 and 7), where the maximum outflow velocities of the absorption trough are  $-200$  and  $-250 \text{ km s}^{-1}$  respectively. The (P Cyg) emission peaks are also usually seen for the Na I D profiles of FUors. At bright phases of Z CMA (e.g. the ‘high state’) the blue absorption wings (shortward 5886 Å and 5890 Å), however, may receive significant contributions from the primary source, because then the continuum of the secondary star is lower than that of the primary. In Jan. and Feb. 2000 the absorption wings extend from  $-200$  to  $-500 \text{ km s}^{-1}$ . The fact that this new wing shows up simultaneously with the maximum in brightness

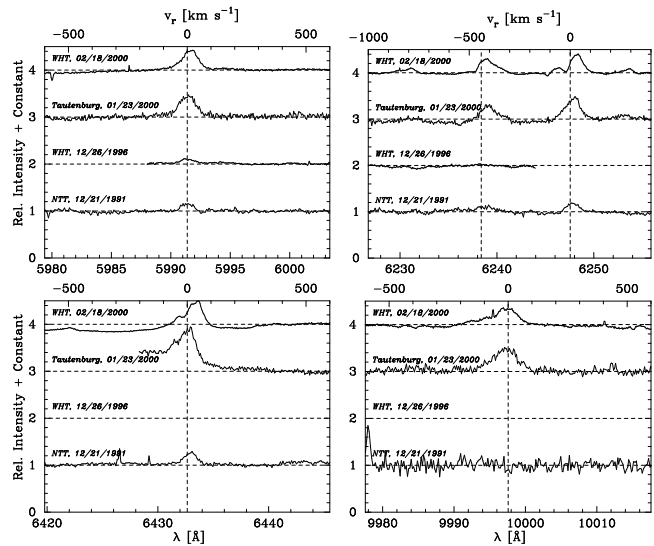


**Figure 7.** Fe II line profile variations in Z CMA between 1991 and 2000. (a) Fe II (46) 5991.38 Å line profile variations, (b) the same for the Fe II (74) 6238.38, 6247.56 Å lines, (c) Fe II (40) 6432.65 Å line, (d) Fe II 9997.58 line. Note the marked increase in Fe II line strength in the Jan. and Feb. 2000 spectra.

of the primary star suggests that this outflow component occurs in the outer atmosphere of the B0 III star. The strength of this wing varies within one month (Fig. 5).

The K I (7698.96 Å) line profile (not shown here) shows the opposite behaviour. In Jan. 2000 it consists of a (broad) emission component and a narrow one (FWHM  $\approx 12 \text{ km s}^{-1}$ ). If the absorption component is interstellar, its EW leads to a K I abundance which is 56 times lower than the Na I abundance derived here. This is 2.8 times lower than the solar abundance of K I. In the WHT spectra of Feb. 2000 a second, broader (FWHM  $\approx 33 \text{ km s}^{-1}$ ) absorption component has appeared, which is blue-shifted by about  $-33 \text{ km s}^{-1}$  with respect to the first component. This broad component, which could be formed in the outer disc or circumstellar region is also present in the spectra of 1991 and 1996. It demonstrates again that during the outburst variability in the outer shell of the primary Be star occurs within a time-scale of less than one month. The Ca II K profile of the Feb. 2000 WHT spectrum (Fig. 8) shows an outflow velocity pattern which is similar to that of the Na I D lines in the same spectrum, but completely different from those of the Fe II (42) and the Balmer lines. This suggests that the Ca II K line is formed over the same outer envelope or disc region as Na I D, which is in line with the comparable excitation potentials of the two lines.

### 4.3 The spectra of Nov./Dec. 1991 ( $V = 9.6^m$ )

#### 4.3.1 The emission lines

Although for Z CMA indications for spectral changes related with brightness variation have been reported previously in the literature (Covino et al. 1984; Finkenzeller & Jankovics 1984; Hessman et al. 1991; Hamann & Persson 1992b; Welty et al. 1992; Teodorani et al. 1997; Garcia et al. 1999), a systematic comparison of red and blue spectra of Z CMA



**Table 3.** Lines detected in the blue spectra of Z CMa (bl = blend). Lines included in square brackets indicate forbidden transitions.

$\lambda$ [Å]	Ident.	WHT, 01/23/2000			BTA, 11/22/1991			WHT, 12/26/1996		
		EW [Å]	FWHM [km s <sup>-1</sup> ]	$v_{\text{out}}$ [km s <sup>-1</sup> ]	EW [Å]	FWHM [km s <sup>-1</sup> ]	$v_{\text{out}}$ [km s <sup>-1</sup> ]	EW [Å]	FWHM [km s <sup>-1</sup> ]	$v_{\text{out}}$ [km s <sup>-1</sup> ]
3933.66	Ca II (1)	-0.96	97	-600				-1.64 <sup>†</sup>	71	-650
4233.17	Fe II (27)	-0.44	80	-106	-0.31	130				
4278.13	Fe II (32)	-0.19	88		-0.17	68				
4290.22	Ti II (41)	-0.28	53	-107	-0.08	67				
4295.17	Fe I (41) +	-0.28	53	-107	-0.07	49				
4295.90	Ti II (20) (bl)									
4306.67	Fe I (42) +	-0.24	44	-98	-0.08	98				
4307.15	Ti II (41) (bl)									
4320.54	Ti II (41) +	-0.22	67	-79	-0.07	62				
4321.95	Sc II (15) (bl)									
4341.77	H $\gamma$	-1.68	158	-704	-0.48	115	-760			
4351.75	Fe II (27)	-0.56	79	-95	-0.18	115				
4358.36	[Fe II]	-0.04	53		-0.03					
4368.25	Fe I (41)	-0.21	61	-61	-0.19	79				
4369.41	Fe II (28)	-0.15	61		-0.09	48				
4374.61	Ti II (93) +	-0.26	69	-103	-0.08	73				
4375.69	Sc II (14) (bl)									
4384.32	Fe II (32)	-0.23	64	-95						
4385.38	Fe II (27)	-0.37	60		-0.16	79				
4395.08	Ti II (19)	-0.41	74	-145	-0.16	126				
4416.83	Fe II (27) +	-0.37	60		-0.17	78				
4417.73	Ti II (40) (bl)									
4468.49	Ti II (31) +	-0.28	51	-114	-0.14	69				
4469.15	Ti II (18) (bl)									
4489.18	Fe II (37)	-0.49	80	-114	-0.18	115				
4491.41	Fe II (37)	-0.52	57		-0.14	138				
4501.37	Ti II (31)	-0.39	59	-118	-0.08	70				
4508.28	Fe II (38)	-0.49	39	-80	-0.27	95				
4515.34	Fe II (37)	-0.66	69	-80	-0.18	80				
4520.22	Fe II (37)	-0.39	51	-93	-0.29	100				
4522.63	Fe II (38)	-0.43	63		-0.4	100				
4533.97	Ti II (50) +	-0.34	59	-92						
4534.17	Fe II (37) (bl)									
4541.52	Fe II (38)	-0.27	59							
4549.47	Fe II (38) +	-0.45	56		-0.32	80				
4549.62	Ti II (82) (bl)									
4555.89	Fe II (37)	-0.41	61		-0.21	76				
4558.66	Cr II (44)	-0.39	56		-0.26	76				
4571.09	Mg I (1) +	-0.26	51	-81	-0.21	118				
4571.97	Ti II (82) (bl)									
4576.33	Fe II (38)	-0.47	72		-0.31	134				
4583.83	Fe II (38)	-0.61	77	-122	-0.51	84				
4588.32	Cr II (44)	-0.26	55		-0.19	92				
4629.34	Fe II (37)	-0.62	66		-0.29	112				
4634.11	Cr II (44) +	-0.14	44		-0.08	95				
4734.12	Fe II (25) (bl)									
4708.66	Ti II (49)	-0.08	54		-0.05	61				
4731.44	Fe II (43)	-0.31	59		-0.11	109				
4805.11	Ti II (92)	-0.32	52	-87	-0.04	40				
4812.35	Cr II (30)	-0.06	51		-0.08	64				
4814.53	[Fe II]	-0.06	55		-0.08	64				
4824.13	Cr II (30)	-0.15	55		-0.04	61				
4861.33	H $\beta$	-5.92	110	-965	-3.03	123	-880			
4876.41	Cr II (30)	-0.11	55		-0.05	47				
4923.92	Fe II (42)	-1.04	85	-186	-0.52	102	-54			
4993.36	Fe II (36)	-0.39	42		-0.18	78				
5018.43	Fe II (42)	-1.73	123	-230	-0.95	120	-48			
5129.14	Ti II (86)	-0.04	33		-0.04	45				
5132.67	Fe II (35)	-0.33	52		-0.08	67				
5158.78	[Fe II]	-0.18	82		-0.13	50				
5169.03	Fe II (42)	-1.91	119		-0.83	77				

**Table 3.** (Continued)

$\lambda$ [Å]	Ident.	WHT, 01/23/2000			BTA, 11/22/1991			WHT, 12/26/1996		
		EW [Å]	FWHM [km s <sup>-1</sup> ]	$v_{\text{out}}$ [km s <sup>-1</sup> ]	EW [Å]	FWHM [km s <sup>-1</sup> ]	$v_{\text{out}}$ [km s <sup>-1</sup> ]	EW [Å]	FWHM [km s <sup>-1</sup> ]	$v_{\text{out}}$ [km s <sup>-1</sup> ]
5188.71	Ti II (70)	-0.26	44		-0.11	78				
5197.57	Fe II (49)	-0.69	66		-0.51	130				
5211.54	Ti II (103)	-0.17	73		-0.11	59				
5226.53	Ti II (70)	-0.47	66		-0.06	52		-0.16	83	
5234.62	Fe II (49)	-0.44	80		-0.23	74		-0.21	59	
5237.37	Cr II (43)	-0.19	58		-0.09	81		-0.09	63	
5261.62	[Fe II]	-0.09	58		-0.05	58				
5269.54	Fe I (15)	-0.45	91					-0.14	60	
5275.99	Fe II (49)	-0.56	58		-0.25	88		-0.15	65	
5279.88	Cr II (43)	-0.11	65		-0.04	58				
5284.09	Fe II (41)	-0.81	65		-0.16	73		-0.07	40	
5305.85	Cr II (24)	-0.14	80		-0.08	40				
5316.61	Fe II (49) +	-1.24	72		-0.64	94		-0.52	91	
5316.78	Fe II (48) (bl)									
5325.56	Fe II (49)	-0.26	72		-0.11	58		0.04	36	
5328.04	Fe I (15)	-0.33	67					0.08	45	
5333.65	[Fe II]	-0.07	43					-0.08	60	
5336.81	Ti II (69)	-0.35	69					0.11	36	
5362.86	Fe II (48)	-0.71	33		-0.37	115		-0.13	43	
5371.51	Fe I (15)	-0.17	57					-0.07	50	
5397.13	Fe I (15)	-0.21	59					-0.11	47	
5405.78	Fe I (15)	-0.15	56					-0.06	38	
5429.67	Fe I (15)	-0.18	47					-0.06	46	
5432.98	Fe II (55)	-0.17	66					-0.06	53	
5434.53	Fe I (15)	-0.08	60					-0.02	18	
5446.92	Fe I (15)	-0.11	47					-0.05	28	
5455.62	Fe I (15)	-0.14	51					-0.04	42	
5497.53	Fe I (15)	-0.11	65					-0.07	46	
5501.48	Fe I (15)	-0.06	46					-0.03	35	
5506.79	Fe I (15)	-0.06	69					-0.04	46	
5534.86	Fe II (55)	-0.53	64					-0.11	48	
5577.34	[O I]	-0.05	73					-0.15	37	
5591.37	Fe II (55)	-0.74	68					-0.09	36	
5754.64	[N II]	-0.05	30					-0.02	40	
6562.81	H $\alpha$	-44.1	191	-920	-16.8	200	-850:	-18.6 <sup>†</sup>	96	-1000

<sup>†</sup> Observed with ESO CAT, 12/16/1996.

in its “low” and “high”-state has not been possible so far. Using previously unpublished spectra from Z CMA in its “low state”, taken from the ESO data-archive, as well as our new data of Z CMA after its Jan. 2000 outburst, we can now compare spectra of Z CMA in its two states over the full spectral range between 4200 and 10000 Å.

From this comparison we draw the following conclusions: (1) The EWs of the Paschen and Ca II (2) emission components in the Jan. 2000 spectra are a factor of 2.0–2.5 larger than the corresponding EWs in the Dec. 1991 spectra. We discuss the consequences of this in Sect. 4.5. The half-widths of the Ca II lines are comparable to those of Jan. 2000 but the outflow velocities are 140–180 km s<sup>-1</sup> lower than in 2000. (2) The EW of the O I (8446 Å) emission line does not seem to increase significantly between the observations in 1991 and 2000 but it is  $\sim 16\%$  larger in Dec. 1987 (Hamann & Persson 1992a) than in Jan. 2000. If this line is excited by Ly $\beta$  pumping, it indicates that it is formed at a location where the Ly $\beta$  fluxes are not significantly different for Dec. 1991 and Jan. 2000. (3) The weak N I emission lines at 8728

and 8683 Å, seen in the Jan. 2000 spectra, are also present in the 1991 NTT spectrum. (4) All obtained spectra contain many emission lines of Fe II, Ti II and Cr II. The analysis of the Fe II lines is given in Sect. 4.6, together with that of the outburst spectra of 1987 and 2000. We also observe the emission lines of Fe I (60). (5) In contrast to the other Fe II emission lines, the Fe II (9997 Å) line, which is extremely strong in the spectra of Jan./Feb. 2000, is not present in the NTT spectrum of 21 Dec. 1991. This line is the strongest line in the near-IR multiplet  $b^4G - z^4F^0$  from which four lines are observed in the spectra of Jan./Feb. 2000 (Table 4) and in which the 9997 Å line is by far the strongest transition. The lines may be pumped directly from Ly $\alpha$  (fluorescence), by cascading from other Ly $\alpha$ -pumped levels, or collisionally pumped from the metastable  $a^4G$  level. These three possible mechanisms correspond with different excitations in the UV (Rodríguez-Ardila et al 2002). Without high resolution UV spectra of Z CMA the method of formation cannot be selected.

**Table 4.** Lines detected in the red spectra of Z CMa (bl = blend, s = single, tr = triplet). Lines included in square brackets are forbidden transitions.

$\lambda$ [Å]	Ident.	Tautenburg, 01/23/2000			WHT, 02/18/2000			NTT, 12/21/1991			WHT, 12/26/1996		
		EW [Å]	FWHM [km s <sup>-1</sup> ]	$v_{\text{out}}$ [km s <sup>-1</sup> ]	EW [Å]	FWHM [km s <sup>-1</sup> ]	$v_{\text{out}}$ [km s <sup>-1</sup> ]	EW [Å]	FWHM [km s <sup>-1</sup> ]	$v_{\text{out}}$ [km s <sup>-1</sup> ]	EW [Å]	FWHM [km s <sup>-1</sup> ]	$v_{\text{out}}$ [km s <sup>-1</sup> ]
5657.87	Sc II (29)	-0.28	38								0.03	43	
5875.62	He I (tr)	2.23	198	-420	0.84	198	-377						
5889.95	Na I (D <sub>1</sub> ) +	4.92	128	-665	4.01	189	-650	2.03	123	-517	3.41	130	-525
5895.92	Na I (D <sub>2</sub> ) (bl)												
5991.38	Fe II (46)	-0.76	77		-0.67	74		-0.25	64		-0.09	48	
6084.11	Fe II (46)	-0.29	109		-0.37	100		-0.07	63				
6113.33	Fe II (46)	-0.06	55					-0.04	67				
6116.61	Fe II (46)	-0.07	55										
6129.73	Fe II (46)	-0.08	66								-0.02	33	
6136.33	Fe II (169)	-0.13	42										
6147.74	Fe II (74) +	-1.23			-0.83			-0.28			-0.21		
6149.25	Fe II (74) (bl)												
6156.41	O I (10)	0.29			0.29	280							
6191.75	Fe I (169)	-0.31	68		-0.33	61		-0.09	50		-0.08	35	
6238.39	Fe II (74)	-0.99	94	-360	-0.65	86		-0.15	73		-0.02	31	
6247.56	Fe II (74)	-1.02	89	-340	-0.84	78		-0.34	77				
6252.56	Fe I (169)	-0.31	68		-0.15	53					-0.08	70	
6300.31	[O I] (1)	-0.44			-4.46 <sup>†</sup>			-0.36			-2.63		
6318.13	Fe I (168)	-0.27	40		-0.13	54		-0.06	52				
6331.95	Fe II (199)	-0.08	88		-0.06	60		-0.08	64				
6347.09	Si II (2)	-0.11											
6363.79	[O I] (1)	-0.07			-0.11	56		-0.07	64		-0.12	66	
6369.46	Fe II (40)	-0.18	61		-0.15	49		-0.15	52				
6371.36	Si II (2)	-0.15	42										
6393.61	Fe I (168)	-0.21	34		-0.18	56		-0.06	52		-0.08	16	
6407.29	Fe II (74)	-0.13	109		-0.12	104		-0.07	60				
6416.91	Fe II (74)	-0.69	85		-0.37	69		-0.2	61		-0.09		
6432.65	Fe II (40)	-1.32	76		-1.26	75		-0.27	55		-0.17	47	
6456.38	Fe II (74)	-1.36	85					-0.35	75				
6482.15	Fe II (199)	-0.17	76		-0.26	51							
6516.81	Fe II (40)	-1.78	84	-330	-1.28	60		-0.58	74		-0.29	43	
6548.04	[N II]	-0.03	17										
6562.81	H $\alpha$	-42.4	200	-1100	-44.1	191	-920	-17.9	120	-1040	-23.4	96	-1000
6583.46	[N II]	-0.02	18		-0.02	22		-0.02	23		-0.03	17	
6678.15	He I (s)	0.67	300					0.06	53				
	He I (s)	-0.03											
6707.81	Li I (1)	0.06	28					0.05	28		0.09		
6717.24	[S II]	-0.13	20		-0.16	60					-0.03		
6726.28	O I (2)	-0.02	75	-200									
6731.31	[S II]	-0.07	20		-0.12			-0.03			-0.05		
6757.21	Si I (8)	-0.01	33										
7005.89	Si I (60)	-0.05	33	-110	-0.04	58							
7017.67	Si I (51)	-0.04	44	-110									
7065.19	He I (tr)	-0.44	280	-430	-0.07	590		<0.04					
7155.16	[Fe II]				-0.10	50		-0.10	85				
7244.85	Si I (51)	-0.04	44	-110				-0.10					
7281.35	He I (s)	-0.65	30					-0.07					
	He I (s)	0.14											
7291.46	[Ca II] (1)	-0.51	56	-77				-0.21	63		-0.21	21	
7310.21	Fe II (73)	-0.35	<95					-0.11	69				
7320.69	Fe II (73)	-0.27	55					-0.11	66				
7323.88	[Ca II] (1)	-0.45	58	-77				-0.11	38		-0.14	30	
7377.91	[Ni II] (2)	-0.04	24	-60	-0.01	27							
7411.87	[Ni II] (2)	-0.08	64					-0.03	31		-0.05	55	
7415.96	Si I (22)	-0.19	100	-100	-0.15	87		-0.04	51				
7449.34	Fe II (73)	-0.32	86		-0.28	78		-0.15	90				
7462.34	Fe II (73)	-0.71	68		-0.57	72		-0.14	48				
7515.84	Fe II (73)	-0.25	60		-0.22	75		-0.08	47		-0.03	71	
7698.96	K I (1)	0.08	12		0.32	15		0.20			0.17		
	K I (1)	-0.08			-0.09			-0.05			-0.08		
7711.73	Fe II (73)	-1.11	82		-0.9	76		-0.25	66		-0.06	50	

**Table 4.** (Continued)

$\lambda$ [Å]	Ident.	Tautenburg, 01/23/2000			WHT, 02/18/2000			NTT, 12/21/1991			WHT, 12/26/1996		
		EW [Å]	FWHM [km s <sup>-1</sup> ]	$v_{\text{out}}$ [km s <sup>-1</sup> ]	EW [Å]	FWHM [km s <sup>-1</sup> ]	$v_{\text{out}}$ [km s <sup>-1</sup> ]	EW [Å]	FWHM [km s <sup>-1</sup> ]	$v_{\text{out}}$ [km s <sup>-1</sup> ]	EW [Å]	FWHM [km s <sup>-1</sup> ]	$v_{\text{out}}$ [km s <sup>-1</sup> ]
7774.17	O I (1)(tr)	2.79	340	450	3.12	300	-250	0.11					
	O I (1)	-0.08			-0.19								
7877.51	Mg II (8)	-0.18	80	-304									
7896.38	Mg II (8)	-0.23		-304				-0.03					
7918.38	Si I (57)	-0.08	66										
7932.35	Si I (57)	-0.08	66										
7944.11	Si I (57)	-0.07	55					-0.06					
8000.12	[Cr II] (1)	-0.21	60										
8012.27	Si I (10)	-0.04	44										
8047.81	Mg I (0)	-0.17	66	-250							-0.05	32	
8201.71	Ca II (13)	-0.15	60		-0.18	87		-0.05			-0.05:		
8213.99	Mg II (7)	-0.03	60		-0.07	78							
8234.64	Mg II (7)	-0.14	60		-0.22	82		-0.14	42				
8248.81	Ca II (13)	-0.27	64	-550	-0.27	83	-250						
8327.11	Fe I (60)	-0.26	60		-0.27	76		-0.12	51				
8345.45	P23 +	-0.53	120					-0.11	39				
8346.13	Mg I (40) (bl)												
8359.00	P22 +	-0.47	128					-0.19	110				
8361.69	He I (bl)												
8374.48	P21	-0.44	80										
8387.78	Fe I (60)	-0.64	80					-0.19	58		-0.19	60	
8392.40	P20	-0.63	100										
8413.32	P19	-0.54	110	-440									
8446.51	O I (4)	-1.37	107		1.82	165	-270	-1.31	120				
8467.25	P17(bl)	-0.58	96	-430	-0.68	111	-255	-0.17	75				
8468.42	Fe I (60)												
8498.02	Ca II (2)	-12.6	107		-10.86	83	-430	-5.51	93	-250	-4.76	101	-282
8502.41	P16(bl)												
8514.10	Fe I (60)	-0.48	62		-0.38	66		-0.07	60		-0.05	44	
8542.10	Ca II (2) +	-14.9:	110	-500	-11.3	81	-460	-5.82	109	-320	-4.95	79	-307
8545.38	P15(bl)												
8598.39	P14	-0.61	89	-420	-0.37	83		-0.19	31				
8629.24	N I (2)	-0.17											
8662.14	Ca II (2) +	-11.8	132	-440	-14.9	73	-500	-5.26	106	-277	-3.59	109	-430
8665.02	P13(bl)												
8683.41	N I (1)	-0.06	55					-0.03	10				
8688.64	Fe I (60)	-0.65	76					-0.12	50		-0.08	50	
8728.89	N I (1)	-0.16	56					-0.18	20				
8750.47	P12	-0.64	93	-430	-0.29	87		-0.32	64				
8806.74	Mg I (7)	-0.84	111	-325	-0.83	101		-0.06	35		-0.04	20	
8824.11	Fe I (60)	-0.51	110		-0.48	66		-0.08	66		-0.05		
8862.78	P11	-0.64	85	-433	-0.51	85		-0.28	52				
8912.07	Ca II	-0.58	106	-415				-0.05	40				
8927.36	Ca II	-0.82	106	-420				-0.06	51				
9014.91	P10							0.32	54				
9063.27	He I (77)	-0.68	150	-435									
9229.02	P9	-0.61	95	-410				0.49	66				
9545.97	P8	-0.82	90	-440									
9854.74	Ca II	-0.43	106										
9997.57	Fe II	-2.02	110	-360	-1.71	110	-380	0.00			0.00		
10049.38	P7	-1.1	88	-420	-0.85	84	-342	0.00			0.00		
10370.51	[S II]				-0.08								
10397.74	[N I]				-0.16								
10459.79	[Ni II]				-0.31								
10501.50	Fe II				-0.09								
10525.14	Fe II				-0.16								
10931.83	P I				-0.23								
10937.83	P6 (P $\gamma$ )				-0.10								

† Observed with ESO 3.6 m, 03/31/2002.

#### 4.3.2 The absorption lines

The strong and broad He I (7065, 6678 and 5876 Å) and O I (7773 and 6156 Å) absorption troughs in the spectra of Jan./Feb. 2000 are much less prominent in the spectra of Dec. 1991. For these lines the same variation was observed by Hessman et al. (1991) between the ‘high state’ and the ‘post-eruption state’. It suggests that the contribution by the FUor dominates the local continuum in Dec. 1991. This is probably also the reason, why the He I (5876 Å) absorption is not present in the Na I D spectrum of Dec. 1991 and Dec. 1996 (Fig. 5). We also find a corresponding reduction in the strength of the He I 7068 Å line, together with the appearance of narrow absorption lines of Fe I at 7068 Å and of Fe I, Ti I, Mn I at 7069–7070 Å and Fe I at 7071 Å. The shape of the O I (7773 Å) profile is shallow around 7772 Å and shows a very small emission peak around 7776 Å. The blue wing of the 5889.95 Na I D<sub>1</sub> line in the 2000, 1996 and 1991 spectra changes in shape. The first absorption component ( $v < 130 \text{ km s}^{-1}$ ) increases in depth between 1991 and Feb. 2000, but decreases between 1996 and 1991. However, the Jan. 2000 spectrum shows a second absorption wing with  $v < 380 \text{ km s}^{-1}$ , which suggests that both lines are formed in the variable outer parts of the envelope or disc atmosphere. The K I (7699 Å) line profile is similar to that of the WHT spectra of Feb. 2000.

### 4.4 The spectra of Dec. 1996 ( $V = 10.2^m$ )

#### 4.4.1 The emission lines

The red WHT spectrum of Dec. 1996, the ESO echelle profiles and the H $\alpha$  profile of Bailey (1998) have been obtained during the deep photometric minimum ( $V \sim 10.2^m$ ) between 1996 and 1999 (Fig. 1). Parts of similar spectra, taken in Jan. 1996 and Jan. 1997 have been published by Teodorani et al. (1997) and Chochol et al. (1998) respectively. Our low resolution spectra of Dec. 1992 also correspond to this brightness. Since the brightness is changing slowly during these years, we have no direct indications for the relative spectral contributions of the components of Z CMa for this phase. However, some hints can be given by comparing these spectra with those of 1991, 2000 and Feb. 1987 (see next section). (1) The ESO profile of H $\alpha$  of Dec. 12 appears similar to the WHT profiles of Dec. 26. The EW of the H $\alpha$  emission has increased slightly with respect to that of 1991. However, Chochol et al. (1998) have found that the daily variations of the H $\alpha$  emission can be considerable so that small changes over long periods do not permit us to draw any conclusions. We also note here that the Paschen emission lines are not detected in the 1996 spectrum, so that the Ca II (2) lines do not have to be corrected for the contribution by the Paschen lines. (2) The ESO profiles of the Ca II (2) lines at 8498 and 8542 Å are very similar to those of the WHT spectrum of Dec. 26. The EWs of the strong emission lines of Ca II (2) and Fe II are lower by a factor of  $\sim 0.6$  than the corresponding EWs measured from the 1991 spectrum. We discuss the consequences for the radii of the emission region in sections 4.5 and 4.6. The profiles of the Ca II lines are similar to those of Dec. 1991. (3) The EW of the Fe I (60) line at 8387 Å is reduced by a factor of 0.85. (4) The EWs of the forbidden emission line of O I (6300 Å) have gradually increased since 1987. For [Fe II] 7155 Å and the [Ca II] lines at 7291

and 7324 Å there also may be an increase with respect to the 1991 data. A probable explanation for this rise is given in Sect. 4.6. (5) The EW of the Ca II K emission varies less than those of the Ca II (2) triplet. It even slightly decreases between 1996 and the outburst stages of 1987 and 2000. This can possibly be due to the fact that the Ca II K line is formed in the outer envelope, in contrast to the Ca II (2) disc lines.

#### 4.4.2 The absorption lines

(1) Although the He I (7065 Å) line has not been observed in the high state of Feb. 1987 and although we observe only the blue half of the He I (6678 Å) line in the 1996 spectrum, we can compare the remaining profiles of these lines in the available spectra. We find that the EWs of these lines are decreasing with decreasing brightness, which indicates a decreasing contribution of the primary B0e star. We can extrapolate this increasing trend and find that in Dec. 1996 the contribution of the primary is at most 10%. We would expect a corresponding increase of the EW for the Li I (6707 Å) line (which is only contributed by the FUor component), but the relatively large errors in line flux due to the weakness of this line in the four spectra prohibit drawing any reliable conclusions regarding an increase in its EW. The decreasing trend is also found for the He I (5876 Å) absorption line. In the 1996 spectrum this line is too weak to be distinguishable in the neighbourhood of the Na I D absorption doublet. (2) The O I (7773 Å) has not been observed in this spectrum (it lies in the gap between order 36 and 37). (3) The Na I D profiles of the ESO and WHT spectra of Dec. 1996 are similar, but the WHT spectrum of Dec. 26 has a higher resolution and shows that the blue components of the lines are double with mean velocities of  $-53$  and  $-128 \text{ km s}^{-1}$ . The Na I D and K I profiles do not differ much from those observed in 1991. The comparison of our 1996 Ca II K profile can be made only with those of the outburst spectra of 1987 and 2000. Our 1991 profile has a higher emission component than the other two profiles. The blue absorption wings of the three profiles are very similar, but in the 2000 spectrum we observe two narrow absorption components at  $-305$  and  $-460 \text{ km s}^{-1}$ , which are difficult to find in the other two spectra, because of the noise.

### 4.5 The Ca II (2) emission lines

In the four high resolution spectra described above, the Ca II (2) triplet emission lines at 8498, 8542 and 8662 Å are (apart from H $\alpha$ ) the strongest lines. Following Hamann & Persson (1992a, b) we shall use our data on these lines as a diagnostic tool to obtain some information about the extended envelope around Z CMa. The profiles of this triplet in the spectra of Feb. 2000, Dec. 1991 and Dec. 1996 are given in Fig. 8. It shows that they have P-Cygni shapes, as is characteristic for many Herbig and T Tauri stars with outflow. As noted by Hamann & Persson (1992a, b) other characteristics of this group are: (a) a tendency for weaker emission lines to be narrower (in order H $\alpha$ , Ca II (2), O I, Fe II), (b) the Ca II (2) peak-flux decreasing in order of increasing wavelength and the EW of the 8542 Ca II line being the largest of the triplet EWs and (c) the presence of Fe I emission lines.

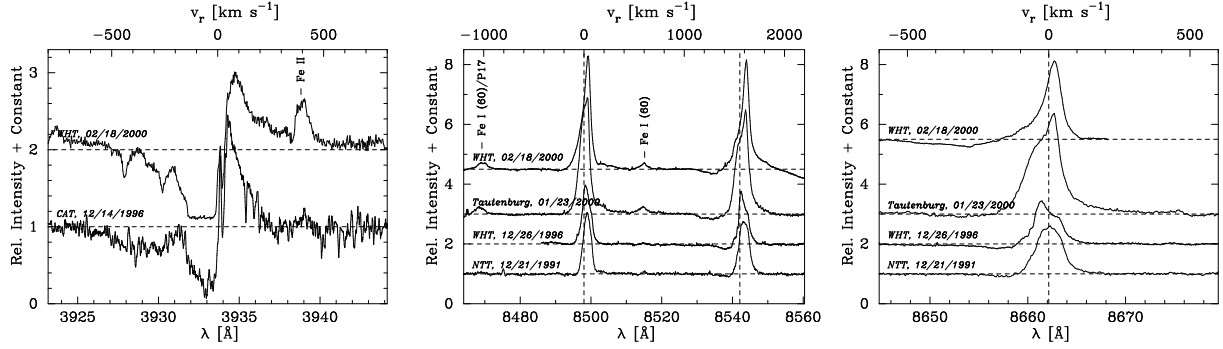


**Figure 8.** Ca II line profile variations in Z CMA between 1991 and 2000. From left to right: (a) the Ca II K line at 3933.66 Å (this spectral range includes Fe II 3938.29 Å, seen in emission in the Feb. 2000 spectrum), (b) the 8498.03 and 8542.09 Å line of the red Ca II (2) triplet (this spectral range also includes the 8514.08 Å Fe I line, and the 8467.8 Å P17/Fe I blend), and (c) the 8662.14 Å line of the Ca II (2) triplet (blended with P13). Again note the marked increase in line strength in the Jan. and Feb. 2000 spectra.

**Table 5.** Ca II (2) line-ratios relative to the 8542 Å line in the spectra of Z CMA, V645 Cyg, FU Ori and V1057 Cyg.

	EW		Peak Height	
	8498/8542	8662/8542	8498/8542	8662/8542
Z CMA (Jan. 2000)	0.85	0.79	1.44	0.73
Z CMA (Feb. 2000)	0.96	–	1.06	–
Z CMA (Dec. 1991)	0.95	0.90	1.18	0.94
Z CMA (Dec. 1996)	0.96	0.73	1.10	0.96
Z CMA (Nov. 1988) <sup>†</sup>	0.87	0.79	1.00	0.86
V645 Cyg <sup>‡</sup>	0.86	0.95	1.18	0.91
FU Ori <sup>†</sup>	0.59	0.88	0.67	0.89
V1057 Cyg <sup>†</sup>	0.65	0.93	0.89	0.92

<sup>†</sup>Determined from Welty et al. (1992). <sup>‡</sup>Determined from Hamann & Persson (1989).

In Table 5 we give the peak and EW ratios of the triplet lines for the five spectra of Z CMA and for those of FU Ori and V1057 Cyg. It is clear that the ratios of both FUors are different from those of Z CMA and V645 Cyg. Our main argument that the observed Ca II (2) emission is produced by the B star component of Z CMA is that the EWs of the Ca II (2) emission lines strongly increase with the increasing continuum contribution by the B-star (10%, 25%, 59%). However, in the spectrum of 1996, where the contribution of the B0-star is only about 10%, Fig. 8 shows a component in the red wing of the Ca II emission profiles, which could be due to the FUor component. We also find a difference in the EWs of the 8540 Å and 8498 Å Ca II (2) emission lines (both  $-3.08$  Å) from the ESO CAT observations, obtained on Dec. 15, 1996, and those ( $-4.95$  and  $-4.76$  Å) observed with the WHT on Dec. 26, 1996. This is consistent with a smaller FWHM ( $93$  km s<sup>-1</sup> for both lines) on Dec. 15 than those from Dec. 26 ( $97$  and  $101$  km s<sup>-1</sup>). These differences could be caused by a variation in the disc of the B-star and/or in the FUor disc.

In our spectra of 2000 and 1991 the (extinction corrected) ratio of the total flux in the Ca II doublet at 8912.7 Å and 8927.4 Å to the total flux of the Ca II (2) triplet is 0.036. Ferland & Persson (1989) have estimated that in the temperature range 5,000–10,000 K, (where Ca II is the dominating ionization stage) it then follows that  $n_e \leq 10^{11}$  cm<sup>-3</sup>.

Because the EW ratio of the triplet members is quite different from the ratio 0.11:1.0:0.56 for the values of  $\log(gf)$  (which should be the ratio if the lines were optically thin) it has been recognised (Polidan & Peters 1976) that the Ca II triplet emission lines are optically thick and saturated. Hamann & Persson (1992b) showed that for  $\tau = 1$  a minimum value for the Ca II column density can be given by  $N(\text{Ca II}) = 2.5 \times 10^{15} \times (v_{\text{turb}}/(50 \text{ km s}^{-1})) \text{ cm}^{-2}$  provided that the line-width is determined by turbulence. For Z CMA this means that  $N(\text{Ca II}) \geq 2.5 \times 10^{15} \text{ cm}^{-2}$  and therefore  $N(\text{H}) \geq 1 \times 10^{21} \text{ cm}^{-2}$ . The condition for saturation is  $\tau \times n_e > 10^{13} \text{ cm}^{-3}$ , so that the optical thickness of the line formation region should be  $\tau \gtrsim 100$  and therefore  $N(\text{Ca II})$  and  $N(\text{H})$  much larger.

Hamann & Persson (1992b) estimate the size of the Ca II emitting region ( $R_{\text{Ca II}}/R_{\star}$ ) from the value of the surface flux of the 8542 Å Ca II line, defined by  $(L_{\text{line}}/L_{\star})\sigma T_{\text{eff}}^4$ . If this line surface flux just equals  $\pi \times \Delta v \times Bv(T_{\text{ex}})$ , where  $\Delta v$  is the full width at half max. of the line and  $T_{\text{ex}}$  is the excitation temperature, they assume that the line emitting region just covers the stellar surface, while larger surface fluxes correspond with in proportion larger surfaces. The authors have calculated the latter function for  $T_{\text{ex}} = 5000$  K,  $v = 25$  and  $250$  km s<sup>-1</sup> and  $T_{\text{ex}} = 10,000$  K and  $v = 250$  km s<sup>-1</sup> and compared (their Fig. 9) the line surface fluxes, derived from the observations of the 8542 Å line for various Herbig and T Tauri stars, with the three calculated limits. For their data of Z CMA (26–28 Dec. 1987) they assumed that it is a single star with spectral type F5. Then the derived 8542 Å line surface flux is equal to the  $T_{\text{ex}} = 5000$  K,  $v = 250$  km s<sup>-1</sup> limit, so that the Ca II emitting region just covers a star with this  $T_{\text{ex}}$ .

From our new data we derived that the Ca II emission is formed in the neighbourhood of the B0 star component of Z CMA. We can scale the line surface flux from that of Hamann & Persson (1992b) by noting that in Jan. 2000 our estimate of the extinction corrected ( $R_{\text{cs}} = 4.2$ ) continuum flux at 8542 Å for the B star component is 0.7 times the corresponding flux of the single F5 star in Dec. 1987. On the other hand the EW of the 8542 Å line in Jan. 2000 is 3.4 times its value, measured in Dec. 1987 and the  $T_{\text{eff}}$  of a B0III star ( $\sim 30,000$  K) is a factor 4.4 larger than that of an F5I ( $\sim 6900$  K) star. In this way we obtain for Jan.

2000 a line surface flux of  $1.71 \times 10^{10}$  erg cm $^{-2}$  s $^{-1}$ . This implies a radius of  $\sim 29.2 R_*$ . Fig. 10 of Hamann & Persson (1992b) then shows that this radius corresponds to the Strömgen radius for a B0 star if  $n_e \sim 8 \times 10^{10}$  cm $^{-3}$ , which is consistent with the value of  $n_e$  estimated from the Ca II doublet and triplet observations above. Ferland & Rees (1988) and Ferland & Persson (1989) have made calculations of the photoionization in the circumstellar region and have shown that at high  $n_e$  the Ca II emission can be produced just beyond the Strömgen radius. Although in this region the dominating ion is Ca III, the emissivity of Ca II appears to be high there because of the high temperatures. For early type B stars the emission of Ca II can arise from extended high density regions from close to the photosphere up to the Strömgen radius, e.g. in and around circumstellar discs.

We can obtain an estimate of the radius of the Ca II disc in Nov./Dec. 1991 by noting that for this epoch the EW of the 8542 Å line is 2.2 times smaller and the extinction corrected ( $R_{cs} = 4.2$ ) continuum flux near the line is 3.4 times smaller than the corresponding values for Jan./Feb. 2000. This means that the line surface flux in Nov./Dec. 1991 will be 0.13 times the line surface flux in Jan./Feb. 2000, so that (if  $T_{ex}$  is the same) it becomes  $2.3 \times 10^{10}$  erg cm $^{-2}$  s $^{-1}$ , which implies an outer disc radius of  $\sim 10.7 R_*$  in Nov./Dec. 1991. In the same way we can use the data of Dec. 1996. For this epoch we estimated that the observed continuum flux of the B0 component is about 10% of the total observed flux. From this we derive that the extinction corrected ( $R_v = 4.2$ ) flux near the 8542 Å line is  $4.17 \times 10^{-12}$  erg cm $^{-2}$  s $^{-1}$ , which is 2.3 times smaller than the corresponding flux in Jan./Feb. 2000. The EW of the 8542 Å emission in the Dec. 1996 spectrum is 3.7 times smaller than the corresponding EW in the Jan./Feb. spectra, so that the line surface flux in Dec. 1996  $\sim 2.0 \times 10^9$  erg cm $^{-2}$  s $^{-1}$  and (if  $T_{ex}$  is the same) the outer disc radius will be  $\sim 9.7 R_*$  in Dec. 1996. We conclude that if  $T_{ex}$  did not change, the outer radius of the Ca II(2) emission region increased during the ‘outburst’ of Jan 2000 with a factor of roughly 3. If  $T_{ex}$  rises the increase in the outer radius will be smaller.

## 4.6 The Fe II emission line spectra

### 4.6.1 Permitted Fe II lines

The EWs of the Fe II emission lines in the spectra of Feb. 1987, Nov/Dec. 1991 and Jan/Feb. 2000 have been measured and are listed in Table 3 and 4. We analysed these line spectra in a statistical way: the self-absorption curve (SAC) method (see Appendix), which is a Curve of Growth version for emission lines. Strictly speaking we should correct the emission EWs for the line absorption, which underlies each emission profile. This can be done for a number of lines, which are observed in absorption in spectra of low activity phases (Finkenzeller & Jankovics 1984; Covino et al. 1984; Welty et al. 1992). However, for the majority of the lines these absorption components are weak and difficult to estimate accurately. In addition part of the absorption components at low brightness phases may be contributed by the FUor component in Z CMA. Therefore we have neglected this correction for all lines.

Because the emission lines contribute very little (at most a few per cent) to the continuum, we can use the

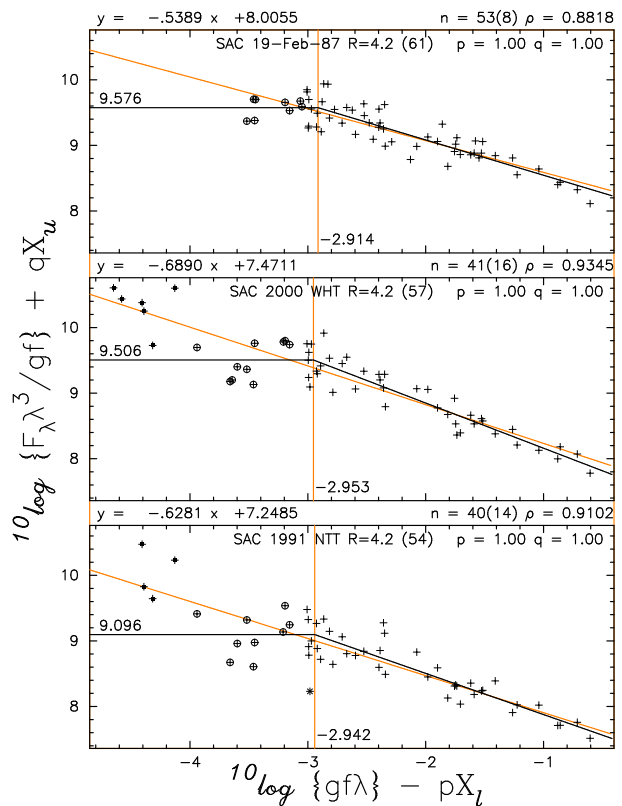


**Figure 9.** Self-absorption curves (SACs) for Fe II lines in the Z CMA spectra from Feb. 1987 (top), Feb. 2000 (middle), and Dec. 1991 (bottom). The + symbols indicate the group of optically thick Fe II lines, the  $\oplus$  symbols indicate the group of optically thin Fe II lines, and the thick drawn lines are linear least square fits to each of these groups. The thin drawn line is a linear least square fit to both Fe II line groups. Typical observational errors are comparable to the size of the plot symbols. The thick crosses (+) in the upper left corners of the middle (SAC 2000) and lower panel (SAC 1991) mark the positions of the forbidden [Fe II] lines. They are not included in the least square fits. The caption of each panel lists the number of optically thick lines ( $n$ ) included in the least square fits, and the correlation coefficient of these fits ( $\rho$ ).

extinction-corrected continuum fluxes derived in the photometric analysis in Sect. 3.2 to transform the EWs into absolute emission line fluxes  $F_\lambda$ . By plotting for each line:  $\log(F_\lambda \lambda^3 / (gf)) + q\chi_u$  versus  $\log(gf\lambda) - p\chi_l$ , with  $\chi_l$  and  $\chi_u$  the excitation energies of the upper and lower terms of the transitions, we obtained a SAC curve for each of the three spectra. From the ‘bending point’ we can obtain a lower limit of the Fe II column density and an upper limit of the radius of the Fe II emission region in each case. In order to calculate  $\log(N_0/g_0)$  we need the value of  $v_0$  in a thin disc, for which we take the thermal velocity, which is about  $2.0 \times 10^5$  cm s $^{-1}$ . In the Appendix it is explained how the values of  $p$  and  $q$  can be obtained from a comparison between the multiplets with common lower terms and of those with common upper terms respectively.

In general the number of lines in a multiplet observed in our spectra was about three, but for several multiplets such as 27, 28, 37, 38, 49, 73 and 74 we observed more lines, up to 8 or 9. The resulting values of  $p$  and  $q$  show a certain spread related with the choice of the multiplet pairs. This

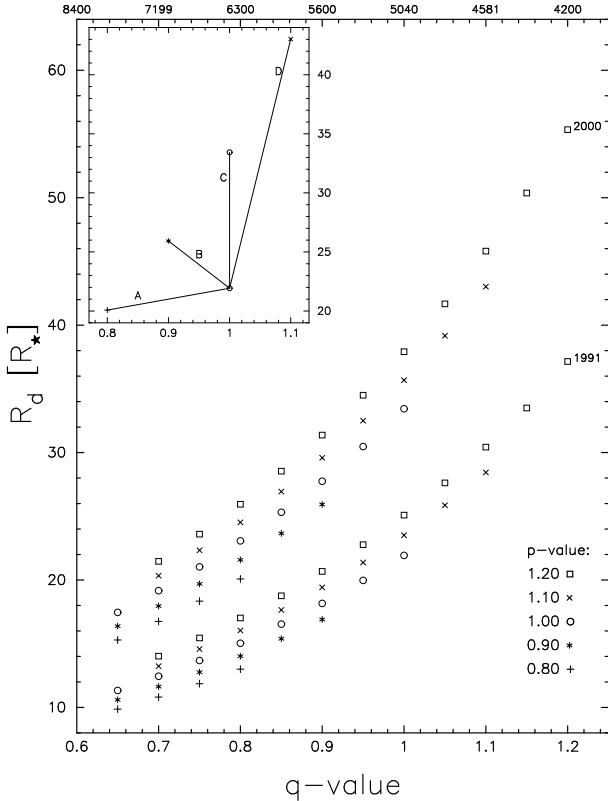


**Figure 10.** Z CMa disc radii as a function of excitation parameter  $q$  for the Feb. 2000 (top) and Dec. 1991 (bottom) Fe II spectra. The insert shows the direction of varying excitation parameters, as discussed in the text.

is partly caused by uncertainties in the EW measurements but perhaps also due to deviations from a thermal excitation mechanism. For the 1987 spectrum we find  $p = 0.9\text{--}1.13$ ,  $q = 0.92\text{--}1.05$ , for the 2000 spectrum  $p = 0.8\text{--}1.10$  and for the spectrum of 1991  $p = 0.7\text{--}1.15$ ,  $q = 0.83\text{--}1.10$ . Since the uncertainties on these numbers are  $\sim 20\%$ , it seems justified to assume that there is no significant difference between the  $(p, q)$  values of the three spectra and that the values of  $p$  and  $q$  are close to 1. If the excitations of the upper and lower terms follow Boltzmann distributions with (excitation) temperatures defined by  $5040/p$  for the lower terms and  $5040/q$  for the upper terms of the transitions, we expect  $p$  to be somewhat larger than  $q$ : perhaps as large as 20%, so that for  $p = 1$  ( $T_l = 5040$  K),  $q$  could be 0.8 ( $T_u = 6300$  K). With these choices for  $p$  and  $q$  we have calculated the SAC curves for the three spectra (e.g. Fig. 9 for  $p = q = 1$ ) We note that the slope of the optically thick part of the curve (at the right side of the bending point), determined by least squares fitting, is around 0.6. Theoretical predictions of the SAC curve for various models of line-formation (Friedjung & Muratorio 1987, Figs. 4c and 4f) indicate that such slope values are consistent with line-formation in winds, confined to a disc.

We derived the upper limits for the disc radius and the lower limits of the column densities of Fe (or  $N(\text{H})$ ) for a range of values of  $p$  and  $q$ , close to 1.0. Fig. 10 gives a survey of the resulting relative disc radii ( $R_d/R_*$ ) for the 1991 spectrum, and for the 2000 spectrum for  $R_{cs} = 4.2$  (for

$R_{cs} = 3.1$  the values of  $R_d/R_*$  are smaller by a factor of 2). Note that, although the exact size of the Fe II emitting region in 1991 and 2000 may be uncertain by a factor 2 or 3 (depending on the assumptions made about the excitation parameters), the ratio of the size of the Fe II emitting region in 1991 and 2000 has a much smaller uncertainty, perhaps  $< 50\%$ . For  $(p, q) = (1, 1)$  when both excitation temperatures are 5040 K, the upper limits of  $R_d/R_*$  for 1991, 2000 and 1987 are 22, 33 and 34. This corresponds to the direction C in the insert of Fig. 10. For the 8542A Ca II (2) emission region we have found (previous section) that the Ca II (2) emission region seems to expand from  $R_{CaII}/R_* = 12$  to  $R_{CaII}/R_* = 29$  between 1991 and 2000. However, if we allow  $(p, q)$  to become lower between 1991 and 2000 the radius will increase less because of the rising upper term excitation temperature (directions B for  $(0.9, 0.9)$  and A for  $(0.8, 0.8)$ ). It is also possible that the excitation temperature decreases between 1991 and 2000 (direction D for  $(1.1$  to  $1.1)$ ). In case D the excitation temperature has decreased by 10%, but the radius of the Fe II disc increases by a factor of 2.0 between 1991 and 2000. For each value of  $(p, q)$  the SAC analysis also provides a lower limit to the column density of Fe II and (with the partition function and the  $N(\text{Fe})/N(\text{H})$  abundance ratio) a corresponding column density of Hydrogen. We used the abundance ratio for the solar environment. For  $(1, 1)$  we find  $N(\text{H}) > 7 \times 10^{23} \text{ cm}^{-2}$  from the spectrum of 1991. In the points A, B, C and D of the spectrum of Jan./Feb. 2000 (Fig. 10) the ratios of  $N(\text{H})$  with respect to the value of  $N(\text{H})$  in  $(1, 1)$  from the 1991 spectrum are 0.28, 0.52, 1.03 and 2.06, respectively. The corresponding ratios of the disc radii upper limits are 0.92, 1.18, 1.52 and 1.96. In this example it seems that the column densities  $N(\text{H})$  increase faster than the disc radii. Since the bending point  $X_0$  of the SAC is independent of continuum flux, the column density  $N(\text{H})$  derived from it will not change for a different choice of spectral type.

#### 4.6.2 The forbidden Fe II lines

In the spectra of Nov/Dec. 1991 and Jan./Feb. 2000 a small number of [Fe II] emission lines with  $\log(gf) > -7.9$  have been found. The line list of Feb. 1987 (Hessman et al. 1991) does not contain such lines, but in the original spectra used by Hessman et al. such lines can also be found. The observed emission fluxes for these lines were treated in the same way as the permitted Fe II lines and marked by filled plot symbols in Fig. 9. The positions of these points are to the left and above the bending points of the curves for the permitted lines. Since these [Fe II] lines are optically thin they are not formed in a dense region such as a disc, but probably in an extended region around the disc. In order to make some estimate of the extension of this region we applied the modified form of the SAC ordinate:  $\log(V/d^2) = Yf - \log(n_0/g_0) + 16.977$  in which  $Yf$  is the normalized emission flux of the line and  $n_0$  is the ground level volume density, which can be estimated from the surface level density and radius, determined from the permitted lines (Baratta et al. 1998).

The results are presented in Table 6, which shows that (for  $p = 1.0$ ,  $q = 1.0$ ) the formation region of the [Fe II] lines is somewhat more extended than the disc, also in the plane of the disc. In the outburst state of Jan. 2000 it has



**Table 6.** Radii of [Fe II] emitting regions in the 1991 and 2000 spectra for  $(p,q)=(1.0,1.0)$ .  $R_d$  = the disc radius. Typical errors in these numbers are  $\sim 20\%$ .

	4385 Å	4815 Å	5158 Å	5261 Å	5333 Å	7155 Å
1991 $R/R_d$	–	2.9	2.7	1.8	–	1.5
2000 $R/R_d$	2.3	2.0	2.3	1.8	2.0	1.2

expanded together with the disc. For the strongest [Fe II] lines the excitation region extends out to nearly three times the upper limit of the disc radius. This result appears to be valid for other values of  $p$  and  $q$  as well.

#### 4.7 The forbidden emission lines of O I, Ca II, N II, N II and S II

There exist at least six recent profiles of the [O I] 6300.3 Å emission in Z CMa: the profile of March 31, 2002, a profile, obtained on Jan 23, 1998 (Garcia et al. 1999), one profile from the WHT spectrum of Dec. 1996, 4 profiles from Jan. 14 to 17, 1997 (Chochol et al. 1998), two profiles from Dec. 20 and 21, 1991 and one profile from Feb. 12, 1987 (Hessman et al. 1991). Fig. 11 shows the profiles for five dates.

Garcia et al. (1999) were able to separate the profiles from the primary (Herbig B0e) and secondary (FUor) star. The deconvolved image in their Fig. 3 indicates that the contribution of the primary to the flux in the central peak of the [O I] emission is at least 2.5 times the contribution of the secondary (FUor) component of Z CMa. This is confirmed by the fluxes of the recovered spectra in their Fig. 2. In addition they showed that the shoulder at the blue side of the line is due to a small (mini-)jet, with a length of  $\sim 1''$  in approximately the direction of the large-scale outflow (Poetzel et al. 1989) and originating from the primary. Garcia et al. suggest that this mini-jet was ejected at the time of the outburst of the primary in Feb. 1987.

In our new [O I] spectra, we note a high-velocity component, extending blueward of the main [O I] emission peak. In the spectrum of 1987 we only observe a single O I peak without shoulder. In all subsequent [O I] 6300 Å profiles a shoulder is present, starting at a distance of  $\sim -600 \text{ km s}^{-1}$  from the peak at 6300.3 Å.

The most recent profile of the [O I] line, taken on March 31, 2002, shows a remarkable increase in the flux of peak and shoulder. The appearance of these broad emission features suggests the sudden development of the high velocity outflow component. We also note the appearance of a second emission peak, centered on  $\sim 6292 \text{ Å}$ , superimposed on the [O I] 6300 Å line profile of Z CMa. This is similar to the second emission peak around 6294 Å in the profile of the [O I] 6300 Å line in the spectrum of PV Cep (Fig. 1 of Corcoran & Ray 1997). This second peak indicates a discrete high velocity component in the outflow, perhaps due to a change in collimation of a jet. An alternative mechanism could be the emission of a discrete line or group of lines. Plausible lines present in the 6290–6305 Å range are the lines of N II, with groupings of lines at 6286–6294 Å and from 6298–6304 Å.

Corcoran & Ray (1997) have noted that a high velocity component in the [O I] 6300 Å profile is a rare phenomenon for Herbig stars. It has only been observed for four stars:

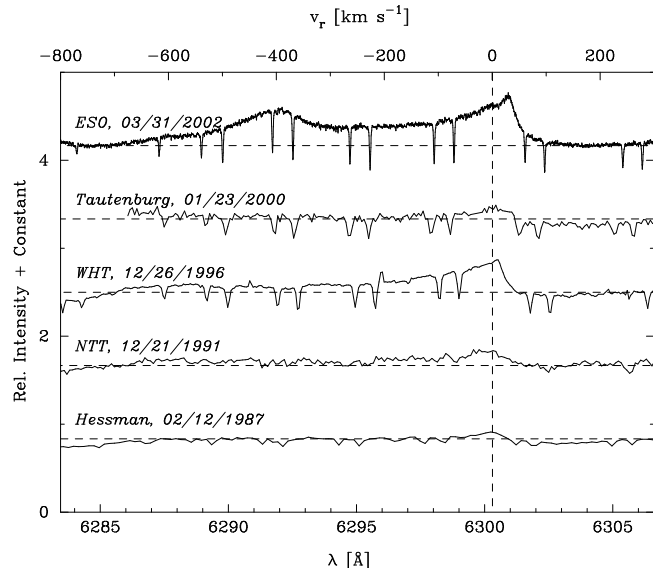


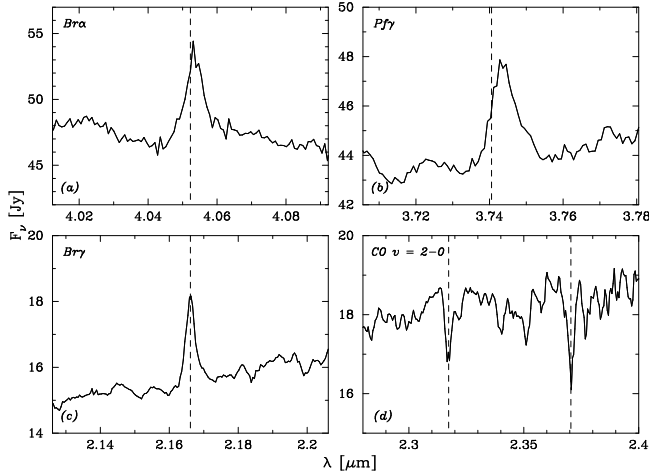
**Figure 11.** Variations in [O I] 6300.2 Å line profile of Z CMa between Dec. 1991 and Feb. 2002. Dashed horizontal and vertical lines again indicate the continuum level and the rest-wavelength. The normalization of the profile of 2000 is somewhat uncertain because it is located near the edge of the echelle order. The narrow absorption lines seen in all spectra are due to telluric water vapour absorption, for which no correction was applied.

V645 Cyg, Z CMa, PV Cep and LkHα 233. These stars are young, embedded stars which are associated with stellar jets and molecular outflows and probably accreting rapidly. The jets form close to the stellar surface and are ejected along the rotation axis of the star. The collimation of such jets within 150–200 AU has been successfully modeled with a stellar or disc-generated wind in a rapidly rotating magnetosphere around such stars. The fact that such high velocity jets are not observed for the majority of the Herbig stars may be caused by differences in the evolution of the collimating magnetic field.

We have also inspected the [Ca II] 7291.46 Å and 7329 Å profiles in the Tautenburg spectrum and in the spectra of Nov./Dec. 1991 and Dec. 1996. It is remarkable that they are similar to the central peak of the [O I] 6300 Å line, but they clearly lack the extended blue shoulder. The same seems to hold for the [O I] 6363 Å, the [S II] 6731 Å, the [N II] 6583 Å and the [O I] 5577 Å profiles, but this is more difficult to verify since the flux in the peak of these lines is three times lower than that of the [O I] 6300 Å line. It is not completely clear whether the central peaks of the [N II] and [S II] lines are mainly due to the primary B0e star. However, it seems convincing that the total flux is dominated by the primary since the [N II] and [S II] fluxes seem confined to the jet direction, which runs through the primary (Poetzel et al. 1989; Garcia et al. 1999). The weakness of the [N II] and [S II] lines does not allow us to obtain reliable profiles. If most of the forbidden lines originate in the neighbourhood of the primary, we can try to use the flux ratios to obtain a rough estimate of the conditions in the far outer atmosphere of the B0e star. Hamann (1994) calculated ratios of various forbidden line fluxes with respect to the line flux of [O I] 6300 Å under the assumptions of coronal ionization equilib-

**Table 7.**  $n_e$  ( $\text{cm}^{-3}$ ) for  $T_e = 13,000$  K. Typical errors in these numbers are  $\sim 30\%$ .

	1996 ( $V = 10.2$ )	1991 ( $V = 9.6$ )	2000 ( $V = 9.2$ )	1987 ( $V = 8.7$ )
[S II] 6732 Å	$8 \times 10^4$	$5 \times 10^4$	$2.0 \times 10^4$	$1.5 \times 10^4$
[Ca II] 7291 Å	–	–	$2.0 \times 10^6$	–
[O I] 5577 Å	$3 \times 10^6$	–	$2.5 \times 10^6$	–
[N II] 6583 Å	–	$3 \times 10^6$	$3.0 \times 10^6$	$2.2 \times 10^6$

**Figure 12.** Fragments of the Z CMa IRTF spectrum of Dec. 2001, showing the lines of Br $\alpha$  (4.05  $\mu\text{m}$ ), Pf $\gamma$  (3.74  $\mu\text{m}$ ), Br $\gamma$  (2.67  $\mu\text{m}$ ) and the CO band-head around 2.3–2.4  $\mu\text{m}$ .

rium and solar abundances. This allows us to estimate  $T_e$  and  $n_e$  from the flux ratios of [N II] (6583 Å), [S II] (6731 Å), [Ca II] (7291 Å) and [O I] (5577 Å) to [O I] (6300 Å). We have used the observed EWs and intrinsic continuum fluxes after circumstellar extinction corrections with  $R_{\text{cs}} = 4.2$ . From the diagrams of Hamann we then obtain for  $T_e = 13,000$  K the values of  $n_e$  in the formation region of the various lines (see Table 7).

For  $T_e = 15,000$  K we find the same trends: (a) for a fixed  $T_e$  the [S II] line comes from the lowest density and therefore at the largest distance from the stellar envelope. (b) the densities decrease when the Be star becomes brighter. This suggests an expansion of the outer region where the forbidden lines are formed.

#### 4.8 The IRTF spectrum

In the IRTF spectrum of Dec. 2001 we observe the emission lines Br $\alpha$  (4.05  $\mu\text{m}$ ), Pf $\gamma$  (3.74  $\mu\text{m}$ ), Br $\gamma$  (2.16  $\mu\text{m}$ ),

**Table 8.** Lines in the IRTF spectrum

$\lambda$ [ $\mu\text{m}$ ]	Ident.	EW [Å]	FWHM [ $\text{km s}^{-1}$ ]	$v_{\text{out}}$ [ $\text{km s}^{-1}$ ]
4.05	Br $\alpha$	−7.75	370	−1600
3.74	Pf $\gamma$	−6.37	545	−1670
2.37	CO (2–0)	4.28	328	–
2.32	CO (2–0)	2.31	328	–
2.17	Br $\gamma$	−5.00	375	−1500

He I (2.06  $\mu\text{m}$ ), Br $\delta$  (1.94  $\mu\text{m}$ ) and absorption in the CO  $v = 2-0$  overtone bands around 2.3  $\mu\text{m}$ . Br $\beta$  is in the observed wavelength-range, but it is obscured by terrestrial atmospheric bands. Fig. 12 shows the profiles of Br $\alpha$ , Pf $\gamma$ , Br $\gamma$  and the CO band. The EWs are given in Table 8. The CO absorption most likely arises in the FUor component of Z CMa (Hartmann et al. 1989). The infrared H I emission lines appear to have similar outflow velocities as their optical counterparts (Fig. 1); they may be related to the inner accretion disk around the Herbig B0 primary. Muzerolle et al. (1998b) have derived empirical relationships between the luminosity of Br $\gamma$  and the accretion rate of T Tauri stars. Our continuum flux at 2.2  $\mu\text{m}$  corresponds to  $K = 4.03^{\text{m}}$ . We therefore have a Br $\gamma$  emission line flux of  $6.0 \times 10^{-12}$   $\text{erg cm}^{-2} \text{s}^{-1}$  or  $\log F(\text{Br}\gamma) = -11.2$ . From Fig. 3 in Muzerolle’s paper we then find by extrapolation that the accretion rate of Z CMa in Dec. 2001 should be  $\sim 2 \times 10^{-5} M_{\odot} \text{yr}^{-1}$ .

#### 4.9 Summary

In the preceding sections we have compared the spectra of the ‘outburst’ phases in Feb. 1987 and Jan./Feb. 2000 with those of the ‘quiescent’ phases Nov./Dec. 1991 and Dec. 1996. The most remarkable distinction between these phases is the appearance of deep absorption lines of He I at 7065, 6678 and 5876 Å and of O I at 7773 Å and 6156 Å in the outburst spectra. We interpret this appearance as a clear indication that the ‘outburst’ occurs in the primary Be component of Z CMa.

The strong similarity between the spectra of Z CMa with those of the class of Herbig Be stars suggests a similar interpretation: the emission lines are formed in a circumstellar disc. Because of the direction of the huge bi-polar jet (large radial velocities in the knots), the association of this outflow with the primary star (Garcia et al. 1999) and the observed polarization of the lines (Whitney et al. 1993), we assume that we are seeing the disc under an angle of at most 40 degrees.

Following Hamann & Persson (1992b) we have used the fluxes of the strong Ca II (2) triplet to estimate the extent of the corresponding excitation region. We found that the outer radius of this region expands from 10  $R_{\star}$  in 1991 and 1996 to  $\sim 29 R_{\star}$  during the outburst in Jan./Feb. 2000. The line profiles of Ca II (2) may indicate that during the faintest phase (Dec. 1996) a small contribution of Ca II emission from the FUor component may be present. The analysis of the Fe II emission multiplets shows a similar expansion of the Fe II region. This expansion is probably somewhat smaller than that of Ca II: 23  $R_{\star}$  in 1991 to 32  $R_{\star}$  in 2000, but 37  $R_{\star}$  in Feb. 1987. [Fe II] emission extends up to twice this distance. Other forbidden lines in the spectra such as [S II], [N II] and [Ca II] correspond to very low values of  $n_e$  and are formed much further away, probably in the bipolar outflow (Poetzel et al. 1989).

The similarity of the Balmer and Paschen outflow velocity pattern with those of the Ca II (2) and Fe II (42) lines (both groups have several outflow components with velocities up to 450–600  $\text{km s}^{-1}$ ) suggests that these lines are formed in the same region. The emission components of Ca II (8542 Å), P11 (8863 Å) and O I (8446 Å) are very similar in profile. Especially in the 1991 spectrum, where the blue absorption wings are less conspicuous, the profiles are very

similar to those of the T Tauri stars BP Tau and UY Aur. Muzerolle et al. (1998) have modeled these BP Tau profiles with a nonrotating, axisymmetric dipole field for magnetic accretion and gave rough relationships between the extinction-free line fluxes of the Ca II (8542 Å), O I (8446 Å) and P11 on one hand and the accretion rate derived from the UV/blue excess continuum (Gullbring et al. 1998) on the other. We have used these relationships to derive for Z CMa accretion rates of  $\log \dot{M} (M_{\odot} \text{ yr}^{-1}) = -4.4$  for the O I and P11 and  $-5.3$  for the Ca II emission lines by extrapolation of Fig. 9 of Muzerolle et al. (1998). From the flux of Br $\gamma$  and Fig. 3 in the paper of Muzerolle et al. (1998b) we obtain by extrapolation that  $\log \dot{M} (M_{\odot} \text{ yr}^{-1}) = -4.7$ . It therefore seems possible that in Z CMa these lines show inflow (magnetospheric accretion) as well as outflow.

Because of the changes in line emission flux and outflow velocities we expect that both flows are different in the various phases of Z CMa. The He I absorption lines have high excitation energies and must therefore be formed close to the star while the O I absorption lines probably have their origin in an extended envelope above and below the disc plane. Most of the emission lines of O I, Ca II, Fe II, Fe I, Cr II, Mg II and the Paschen lines form in the disc. Na I D, K I and Ca II K are formed further out in the envelope. The Ca II K absorption pattern shows similarities with those of the Na I D lines. These lines may receive contributions from the envelope of the FUor component as well. However, it seems highly probable that the variations in these profiles also reflect changes in the outer envelope of the primary Be star during the outburst phases.

Two new phenomena have been observed in connection with the outburst of Jan. 2000: the appearance of a strong Fe II 9997 Å emission line and of an extended blue shoulder in the [O I] 6300 Å emission profile in 2002. The origin of the first emission is not yet clear. It is possible that Ly $\alpha$  fluorescence is the mechanism for its production. The emission profiles of the [O I] 6300 Å and the [Ca II] 7291, 7323 Å doublet profiles show a gradual growth in EW since Dec. 1987. The blue shoulder in the [O I] 6300 Å profile, detected two years after the outburst of Jan. 2000 is possibly caused by a sudden change in the collimation process of the mini-jet, which could have been ejected in Feb. 1987.

## 5 DISCUSSION

The spectrum of Z CMa in its normal state has been satisfactorily explained by Hartmann et al. (1989), and Welty et al. (1992) in terms of that of a rotating, optically thick, accretion disc. From a total luminosity of 3000 L $_{\odot}$  Hartmann et al. (1989) derived for  $v \sin i \sim 100 \text{ km s}^{-1}$  an inner disc radius of 16 R $_{\odot}$  and an accretion rate of  $\sim 10^{-3} M_{\odot} \text{ yr}^{-1}$  to a central star of 1–3 M $_{\odot}$  and radius  $\sim 9$ –16 R $_{\odot}$ . However, during the outburst of Feb. 1987 (Hessman et al. 1991) the spectrum was completely different and the observers of this high state could not explain it in terms of the same or an adapted model. It were the spectropolarimetric observations of Whitney et al. (1993) that showed that the usually small contribution of the infrared primary star to the visual continuum could rise to  $\sim 66\%$  of the total continuum flux during the outburst of 1987. Whitney et al. (1993) have noted that in this high state the emission spectrum of

Z CMa is very similar to that of the Herbig Be star MWC 1080. The agreement is not limited to the emission lines but also to the profile of the Na I D line (Finkenzeller & Mundt 1984). Similar to Z CMa, the He I lines at 6687 and 5876 Å of MWC 1080 are in absorption (Yoshida et al. 1992).

We also note a strong spectral similarity with the luminous young object V645 Cyg (Hamann & Persson 1989), which has been classified as O8. Especially the broad Fe II 9997 Å emission line and the broad O I (7774 Å) absorption line together with a relatively weak O I (8446 Å) emission is very similar to the high state of Z CMa. This indicates an important role of Ly $\alpha$  and Ly $\beta$  emission in both stars. A difference is that the He I (6678 Å) P-Cygni profile of V645 Cyg has a more prominent emission component than its counterpart in Z CMa. This may point to a somewhat hotter inner disc. Another feature which both objects have in common is the high velocity component of the [O I] 6300 Å emission profile (see below).

The spectrum of Z CMa has also been compared with the rich emission line spectrum of V380 Ori. However, the spectrum of V380 Ori (Rossi et al. 1999) shows some marked differences with those of Z CMa and MWC 1080. Its He I lines at 6678 and 5876 Å are generally in emission, but occasionally in absorption. It has been suggested by Rossi et al. and others that this may indicate the presence of a chromosphere or a hot accretion spot close to the stellar surface. Its O I (7773 Å) line is also in emission, which is not unusual for various early A-type Herbig stars, such as AB Aur (A0e), HD 163296 (A2e) and BD +61°154 (B8e) (Felenbok et al. 1988). An independent argument for a classification of V380 Ori as a B9–A0e star is the cut-off of the ultraviolet continuum near 1300 Å in the low resolution IUE spectra of V380 Ori (Rossi et al. 1999).

The spectral type of the Z CMa primary component was found to be close to B0e (Sect. 4.2). From  $V_0 = 6.05^m$  and a distance of 1050 pc we find an absolute magnitude  $M_V = -4.1^m$ , which may indicate a classification B1–2 III. In Sect. 3.2 we have derived the luminosities of the primary component for Nov. 21, 1991 (the date of the polarization spectra of Whitney et al. 1993) and Feb. 20, 1987 (the ‘high state’ of Z CMa). The results for three assumptions for  $R_{cs}$  (the ratio of total to specific absorption of the circumstellar envelope): 3.1, 4.2 and 6.0 are given in Table 2.

It may be interesting to compare the temperatures and the de-reddened luminosities of this table with recent calculations of the pre-main sequence evolution of young massive stars by Behrend & Maeder (2001). The comparison shows that in the high state for  $R_{cs} = 3.1$  and  $R_{cs} = 4.2$  the emission line star can be identified as a pre-main sequence star, since then it can be modelled as a 16 M $_{\odot}$  B0 III star ( $T_{\text{eff}} \sim 31,600 \text{ K}$ ) on the birthline with an age of  $3 \times 10^5 \text{ yr}$  and a luminosity of 47 L $_{\odot}$  and radius 7.6 R $_{\odot}$ . For  $R_{cs} = 6.0$  the luminosity is too high and the position of the star is above the birthline and, in order to be observable, it should be a post main sequence star. From the post main sequence evolutionary calculations of Schaller et al. (1992) we find that it could be 20 M $_{\odot}$  B0 III star with an age of  $\sim 6.6 \text{ Myr}$ . This is close to the estimated ages of the nearby B0e stars HD 53367 and HD 53755 (paper II). On the other hand the parameters of the inner star of the FUor component, estimated by Hartmann et al. (1989), correspond to a 3 M $_{\odot}$  star with a radius of 7 R $_{\odot}$ , an effective temperature of 5000 K,

a luminosity of  $28 L_{\odot}$  and an age of  $3 \times 10^5$  yr. Its position in the HR diagram is just below the birthline. In this case both components of Z CMA have the same age and could have been born together.

Recently Yorke & Sonnhalter (2002) have published evolutionary models for star formation in which radiative acceleration of dust grains has been taken into account in the radiative transfer. The results of the evolution depend on the opacity law of the dust. For a frequency-dependent opacity law due to a mixture of two dust components with specified size distributions the evolution leads to the formation of massive stars via disc accretion with a massive bipolar jet. For a ‘gray’ opacity law, however, the evolution proceeds without bipolar jet and results in a thin, disc-like object. Since in these models the birthline is raised by a factor ten (for B0 stars) with respect to the previous models, they can easily interpret the Z CMA primary luminosity of Feb. 1987 with  $R_{cs}$  up to 6 as the luminosity of a pre-main sequence star. The paper shows 2-dimensional models of the immediate neighbourhood of the stars for a wide grid of masses, ages and luminosities.

For our case of  $3.1 \times 10^5 L_{\odot}$  (Table 2,  $R_{cs} = 6$ ) we are not far from a model of a  $38 M_{\odot}$  star, close to the birthline with an age of  $4 \times 10^4$  Myr (model F120, 11c). For this age the model predicts a mass accretion rate smaller than  $10^{-4} M_{\odot} \text{ yr}^{-1}$ , which is consistent with our estimate from the Br $\gamma$  flux in Sect. 4.8. Similar to Z CMA, the 2-dimensional model shows an indication of an accretion disc and of a strong bipolar outflow. The dynamical time scale of  $2\text{--}3 \times 10^4$  years for the ‘slow’ knots (Poetzel et al. 1989) in the bipolar jet fits within the model age of this B0e star.

For ages comparable with those of the B0 star models the FUor component could correspond to a ‘gray’ opacity model such as G60 of Yorke & Sonnhalter (2002) but for a lower luminosity and mass than calculated in their Table 4. Such a model does not develop a bipolar outflow, but evolves to a disc-like structure, perhaps a FUor. In this case we may have a simultaneous birth of the Z CMA components. This is in agreement with the polarization results of Fischer et al. (1998), who came to the conclusion that both components must have had a common formation history. However, the models by Yorke & Sonnhalter imply a difference in grain properties for the regions in which the B0 and the FUor component are formed. Because the present rotation velocity of the B0 component and its previous evolution are not known we cannot be certain of the evolutionary age, but so far it seems that the age estimates of Z CMA with both models are much lower than those of the other massive stars in the CMA R1 complex, which are closer to the main sequence (paper I, II). How can the low age of Z CMA be fitted in the evolutionary history of CMA R1? The formation must be related to fragmentation in the high density in the dark cloud S296 where Z CMA is situated, but so far it remains unclear which process initiated the contraction in the cloud which started the recent star formation.

Apart from the long-term evolution of Z CMA there remain a number of questions concerning the recent behaviour of the two components:

(1) The cause of the photometric variability: At least two types of variabilities have been observed: (a) irregular low amplitude variations, which seem on the average to follow density variations in the circumstellar dust. V.S.

Shevchenko made an extensive search of periodicities in the *UBVR* photometry, collected by the ROTOR program during the years 1981–1998. A period of 393 days was found with an amplitude of  $0.3^m$  in  $U - B$  and  $0.08^m$  in  $B - V$ . The underlying cause of such a periodicity is not yet known but pulsational instability may be a possibility. (b) Strong and fast rises in brightness (outbursts) around 1968 ( $\Delta V \sim 0.7^m$ ), 1987 ( $\Delta V \sim 0.6^m$ ) and 2000 ( $\Delta V \sim 1.2^m$ ). We have now some indications that the second outburst has caused the ejection of the mini-jet emitting [O I] 6300 Å (Garcia et al. 1999), similar to those observed in other young emission-line objects such as PV Cep, V645 Cyg and LkH $\alpha$  233 (Corcoran & Ray 1997). The third outburst (in Jan. 2000) probably caused a change in the [O I] 6300 Å profile (see Fig. 11) which could be due to a change in the collimated outflow. The outbursts therefore could be related to changes in the upper layers of the stellar interior, which entail changes in the magnetic field configuration. Such changes could have an internal origin or be induced by an origin from outside the star, e.g. by tidal interaction during approaching component stars. The latter possibility (Bonnell & Bastien 1992) can be ruled out by the following argument: The projected distance between the components of Z CMA is  $\sim 0.1''$  which at a distance of 1050 pc corresponds to  $\sim 105$  AU. This is seen in projection and therefore the minimum distance of the components. A minimum for the period can then be estimated from Keplers law. For  $M_1 = 38 M_{\odot}$  and  $M_2 = 3 M_{\odot}$ , we find a minimum period of 168 yrs. This is too large for an observed recurrence of outbursts at a timescale of once per 10–12 yrs. The remaining possibilities are that the primary star has a, as of yet undetected, close binary component or that the outbursts are induced by variations in the star itself.

(2) According to Garcia et al. (1999) the direction of the mini-jet coincides with that of the large bi-polar outflow of Z CMA and the outflow is driven by the massive B0 component. Also the evolutionary models of Yorke & Sonnhalter (2002) predict large bi-polar outflows during the formation of massive stars. However, Velázquez & Rodríguez (2001) claim that the large bipolar outflow coincides with the radio-jet through the FUor component. If this is true, the question remains how the cavity in the cocoon is formed, through which we observe the optical spectrum of the B-star. One possibility is that it has been formed in the past when the infrared source approached the FUor. Somehow the direction of the bipolar outflow is then conserved in the infrared source and transferred to the mini-jet.

## ACKNOWLEDGMENTS

The authors are indebted to Drs. H. van Winckel and G. Meeus for obtaining the Dec. 1996 spectrum of Z CMA at the WHT, and to Dr. Lee Hartmann for sharing the original spectra of Z CMA during the 1987 outburst. We also would like to thank the service-observers at the ING group (especially Dr. I. Skillen and Dr. B. Garcia) for their excellent work in obtaining the Feb. 2000 WHT service-mode observations of Z CMA, and the observers of the ROTOR photometric program at Mt. Maidanak for their quick notification of the outburst of Dec. 1999. We also would like to thank Dr. L.N. Berndnikov for obtaining *UBVRI* photometry of

Z CMa during his stay at the South African Astronomical Observatory in March 2002. One of us (H.T.) thanks in particular Dr. R. Viotti and Dr. M. Friedjung for helpful discussions concerning the application of the SAC method. We also thank the referee, Dr. B. Reipurth, for his constructive remarks which improved content and presentation of the manuscript. This research has made use of the Simbad data base, operated at CDS, Strasbourg, France. Atomic data used in this study were extracted from the Atomic Line List maintained at <http://www.pa.uky.edu/~peter/atomic/>.

## REFERENCES

- Bailey J., 1998, MNRAS 301, 161  
 Baratta G.B., Friedjung M., Muratorio G., Rossi V., Viotti R., 1998, “The Self-Absorption-Curve-Method - A User’s Manual” (<http://www.rm.iasf.cnr.it/uvspace/>)  
 Barth W., Weigelt G., Zinnecker H., 1994, A&A 291, 500  
 Behrend R., Maeder A., 2001, A&A 373, 190  
 Bonnell I., Bastien P., 1992, ApJ 401, L31  
 Brand J., Wouterloot J.G.A., 1988, A&AS 75, 117  
 Carpenter J.M., 2001, AJ 121, 2851  
 Chochol D., Teodorani M., Strafella F., Errico L., Vittone A.A., 1998, MNRAS 293, L73  
 Corcoran M., Ray T., 1997, A&A 321, 189  
 Covino E., Terranegra L., Vittone A.A., Russo G., 1984, AJ 89, 1868  
 de Winter D., van den Ancker M.E., Maira A., Thé P.S., Tjin A Djie H.R.E., Redondo I., Eiroa C., Molster F.J., 2002, A&A 380, 609  
 Evans N.J., Balkum S., Levreault R.M., Hartmann L., Kenyon S., 1994, ApJ 424, 793  
 Faraggiana R., Gerbaldi M., van ’t Veer C., Floquet M., 1988, A&A 201, 259  
 Felenbok P., Czarny J., Catala C., Praderie F., 1988, A&A 201, 247  
 Ferland G.J., Persson S.E., 1989, ApJ 347, 656  
 Ferland G.J., Rees M.J., 1988, ApJ 332, 141  
 Fernie J.D., 1983, PASP 95, 782  
 Finkenzeller U., Mundt R., 1984, A&AS 55, 109  
 Finkenzeller U., Jankovics I., 1984, A&AS 57, 285  
 Fischer O., Stecklum B., Leinert C., 1998, A&A 334, 969  
 Friedjung M., Muratorio G., 1987, A&A 188, 100  
 Garcia P.J.V., Thiébaud E., Bacon R., 1999, A&A 346, 892  
 Garrison L.M., 1978, ApJ 224, 535  
 Gullbring E., Hartmann L.W., Briceno C., Calvet N., 1998, ApJ 492, 323  
 Haas M., Christou J.C., Zinnecker H., Ridgway S.T., Leinert C., 1993, A&A 269, 282  
 Hamann F., Persson S.E., 1989, ApJ 339, 1078  
 Hamann F., Persson S.E., 1992a, ApJS 82, 285  
 Hamann F., Persson S.E., 1992b, ApJS 82, 247  
 Hamann F., 1994, ApJS 93, 485  
 Hartmann L.W., Kenyon S.J., Hewett R., Edwards S., Strom K.M., Strom S.E., Stauffer J.R., 1989, ApJ 338, 1001  
 Hessman F.V., Eislöffel J., Mundt R., Hartmann L.W., Herbst W., Krautter J., 1991, ApJ 370, 384  
 Jaschek M., Jaschek C., Andrillat Y., 1993, A&AS 97, 781  
 Kastner S.O., 1999, A&A 351, 1016  
 Kenyon S.J., Hartmann L.W., Imhoff C.L., Cassatella A., 1989, ApJ 344, 925  
 Koresko C.D., Beckwith S.V.W., Ghez A.M., Matthews K., Neugebauer G., 1991, AJ 102, 2073  
 Kurucz R.L., 1981, Semi-empirical Calculations of *gf* values IV: Fe II, Smithsonian Astrophys. Obs. Rep. 390, 1  
 Lamzin S.A., Teodorani M., Errico L., Vittone A.A., Kolotilov E.A., Miroshnichenko A.S., Yudin R.V., 1998, Astron. Reports 42, 630  
 Merrill P.W., 1927, ApJ 65, 291  
 Mihalas D., 1966, ApJS 13, 1  
 Millan-Gabet R., Monnier J.D., 2002, ApJ 580, L167  
 Muratorio G., Viotti R., Friedjung M., Baratta G.B., Rossi C., 1992, A&A 258, 423  
 Muzerolle J., Hartmann L.W., Calvet N., 1998a, AJ 116, 455  
 Muzerolle J., Hartmann L.W., Calvet N., 1998b, AJ 116, 2965  
 Poetzel R., Mundt R., Ray T.P., 1989, A&A 224, L13  
 Polidan R.S., Peters G.J., 1976, in “Be and Shell Stars”, IAU Symp. No. 70, eds. A. Slettebak, Reidel, Dordrecht, p. 59  
 Rayner J.T., Toomey D.W., Onaka P.M., Denault A.J., Stahlberger W.E., Vacca W.D., Cushing M.C., Wang S., 2003, PASP 155, 362  
 Rodríguez-Ardila A., Viegas S.M., Pastoriza M.G., Prato L., 2002, ApJ 565, 140  
 Rossi C., Errico L., Friedjung M., Giovannelli F., Muratorio G., Viotti R., Vittone A., 1999, A&AS 136, 95  
 Schaller G., Schaerer D., Meynet G., Maeder A., 1992, A&AS 96, 269  
 Schmidt-Kaler Th., 1982, “Landölt-Bornstein Catalogue”, VI/2b, Springer Verlag  
 Slettebak A., 1986, PASP 98, 867  
 Shevchenko V.S., 1989, “Herbig Ae/Be Stars” (Tashkent: Uzbek. Acad. Sci.)  
 Shevchenko V.S., Ezhkova O.V., Ibrahimov M.A., van den Ancker M.E., Tjin A Djie H.R.E., 1999, MNRAS 310, 210 (Paper I)  
 Teodorani M., Errico L., Vittone A.A., Giovannelli F., Rossi C., 1997, A&AS 126, 91  
 Thiébaud E., Bouvier J., Blazit A., Bonneau D., Foy F.C., Foy R., 1995, A&A 303, 795  
 Tjin A Djie H.R.E., van den Ancker M.E., Blondel P.F.C., Shevchenko V.S., Ezhkova O.V., de Winter D., Grankin K.N., 2001, MNRAS 325, 1441 (Paper II)  
 Velázquez P.F., Rodríguez L.F., 2001, Rev. Mex. AA. 37, 261  
 Viotti R., Rossi C., Muratorio G., 1998, A&AS 128, 447  
 Voshchinnikov N.V., Farafonov V.G., 1993, Ap&SS 204, 19  
 Welty A.D., Strom S.E., Edwards S., Kenyon S.J., Hartmann L.W., 1992, ApJ 397, 260  
 Whitney B.A., Clayton G.C., Schulte-Ladbeck R.E., Calvet N., Hartmann L.W., Kenyon S.J., 1993, ApJ 417, 687  
 Yorke H.W., Sonnhalter C., 2002, ApJ 569, 862  
 Yoshida S., Kogure T., Nakano M., Takematsu K., Wiramihardja S.D., 1992, PASJ 44, 77

## APPENDIX A: THE SELF-ABSORPTION CURVE (SAC) METHOD

The observation of many multiplets of emission lines of Fe II, Ti II and Cr II (Table 4) allows us to derive some information concerning the formation regions of these lines with the help of an emission curve of growth method. The method is based on the analysis of the self-absorption curve (SAC) which was developed by Friedjung & Muratorio (1987) and has been successfully applied to various Fe II emission line spectra (e.g. Muratorio et al. (1992) for the case of KQ Pup)<sup>§</sup>. A manual for the use of the method has been written by Baratta et al. (1998).

The SAC curve describes the relation between the line

<sup>§</sup> An independent derivation of the SAC method has been given by Kastner (1999)

strength and optical depth of emission lines in a multiplet. This relation can be empirically determined by plotting  $\log(F_\lambda \lambda^3 / gf)$  (where  $F_\lambda$  is the normalised absolute line flux and  $gf$  is the oscillator strength of the line) versus  $\log(gf)$  (which is the optical depth at line-center up to an additional constant) for the various lines of each multiplet. In these empirical plots the lines through the points of each multiplet should be parallel to each other and to the still unknown theoretical SAC function  $Q(\tau)$ , which should be zero for  $\log \tau < 0$  and should decrease approximately linearly for  $\log \tau > 1$ . The emission lines in the horizontal part of the SAC (with  $\log \tau < 1$ ) are optically thin, whereas those in the decreasing part are increasingly optically thick. For the various Fe II emission lines the oscillator strength and excitation energies have been taken from the tables of Kurucz (1981).

The various curves for multiplets with common upper terms<sup>¶</sup> will be parallel and shifted by  $p\chi_l$  in horizontal direction with respect to each other, whereas those with common lower terms<sup>||</sup> will be shifted by  $q\chi_u$  in vertical direction with respect to each other. Here  $\chi_l$  and  $\chi_u$  are the excitation potentials of the lower and upper terms in the transitions and  $p$  and  $q$  are the values of  $5040/T_l$  and  $5040/T_u$ , where it is assumed that the levels have Boltzmann-type populations with excitation temperatures  $T_l$  and  $T_u$  for the lower and upper terms respectively. Since we know the excitation potentials, we can determine the values of  $p$  and  $q$  from the horizontal and vertical shifts and therefore the Boltzmann temperatures.

By plotting  $Y = \log(F_\lambda \lambda^3 / gf) + q\chi_u$  versus  $X = \log(gf\lambda) - p\chi_l$  for the lines of each multiplet, we can obtain one common empirical SAC curve for the Fe II lines. The value  $X_0$  on the X-axis, at which the empirical SAC curve starts to decrease for increasing  $X$ , gives us  $\log(N_0/g_0)$  up to constant  $\log v_o + 1.576$  (in cgs units), where  $v_o$  is the line broadening velocity and  $N_0$  is the ground state column density of Fe II from which the total Fe and H column densities can be estimated. From the normalized emission line flux  $Y_0$  in this point  $X_0$ , where the empirical SAC curve starts to decrease, it is then possible to estimate the extension of the surface area  $S$  of the emission region (perpendicular to the line of sight) using  $\log(S/d^2) = Y_0 - \log(N_0/g_0) - w + 16.977$ , where  $d$  is the distance to the source (here 1050 pc) and  $w = -(p - q) \times (\chi_l + \chi_u)/2$ . An example of the empirical SAC curves of Fe II emission lines of three spectra of Z CMa (observed in Feb. 1987, Jan. 2000 and Nov. 1991) is given in Fig. 9.

For spectra with only optically thick lines, one can only obtain the decreasing part of the SAC curve, so that the values of  $X_0$  and  $Y_0$  have to be estimated. The method then only gives a lower limit to the column density and an upper limit to the extension of the emission line region. On the

other hand the method can be applied to optical thin forbidden lines, to derive a characteristic volume (or radius) of their emission region. Finally the slope of the decreasing part of the theoretical SAC curve has been shown to depend on the dynamical conditions in the emission region (Friedjung & Muratorio 1987). In our case of Z CMa the slope is close to  $-0.6$ , which may indicate that the Fe II lines are formed in a disc wind (Fig. 4f in Friedjung & Muratorio 1987).

This paper has been produced using the Royal Astronomical Society/Blackwell Science L<sup>A</sup>T<sub>E</sub>X style file.

<sup>¶</sup> In the visual part of the spectrum Fe II multiplets with common upper terms are: 27, 38, 48 and 73 ( $^4P(^5D)^4D$ ), 28, 32, 37, 49 and 55 ( $^4P(^5D)^4F$ ), 26,42 and 36 ( $^4P(^5D)^6P$ ), 29 and 74 ( $^4P(^5D)^4P$ ), and 41 and 46 ( $^4P(^5D)^6F$ ).

<sup>||</sup> In the visual part of the spectrum Fe II multiplets with common lower terms are: 27, 28 and 29 ( $D^6S(^3P)^4P$ ), 36, 37 and 38 ( $D^6S(^3F)^4F$ ), 40, 41, 42 and 43 ( $D^5S^2(^7S)^6S$ ), 46, 48 and 49 ( $D^6S(^3G)^4G$ ) and 72, 73 and 74 ( $D^6S(^3D)^4D$ ).